SANTA ANA ASSOCIATED OFFSHORE FOG:
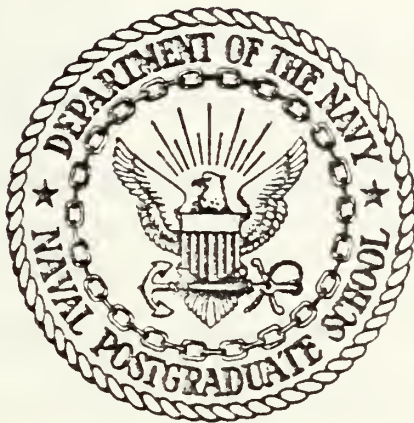# FORECASTING WITH A SEQUENTIAL MODEL.

Douglas Allen Backes

NAVAL POSTGRADUATE SCHOOL
Monterey, California

THESIS

SANTA ANA ASSOCIATED OFFSHORE FOG:
FORECASTING WITH A SEQUENTIAL MODEL

by

Douglas Allen Backes

September 1977

Thesis Advisor: Dale F. Leipper

T179909

REPORT DOCUMENTATION PAGE		READ INSTRUCTIONS BEFORE COMPLETING FORM
1. REPORT NUMBER NPS-68LR77091	2. GOVT ACCESSION NO.	3. RECIPIENT'S CATALOG NUMBER
4. TITLE (and Subtitle) Santa Ana Associated Offshore Fog: Forecasting with a Sequential Model		5. TYPE OF REPORT & PERIOD COVERED Master's Thesis; September 1977
		6. PERFORMING ORG. REPORT NUMBER
7. AUTHOR(s) Douglas Allen Backes in conjunction with Dale F. Leipper		8. CONTRACT OR GRANT NUMBER(s)
9. PERFORMING ORGANIZATION NAME AND ADDRESS Naval Postgraduate School Monterey, California 93940		10. PROGRAM ELEMENT, PROJECT, TASK AREA & WORK UNIT NUMBERS 61153M; N00019-77-WR-71012
11. CONTROLLING OFFICE NAME AND ADDRESS Naval Air Systems Command, 370C Washington, D.C. 20360		12. REPORT DATE September 1977
		13. NUMBER OF PAGES
14. MONITORING AGENCY NAME & ADDRESS(if different from Controlling Office) Naval Postgraduate School Monterey, California 93940		15. SECURITY CLASS. (of this report) Unclassified
		15a. DECLASSIFICATION/DOWNGRADING SCHEDULE

16. DISTRIBUTION STATEMENT (of this Report)

Approved for public release; distribution unlimited

17. DISTRIBUTION STATEMENT (of the abstract entered in Block 20, if different from Report)

18. SUPPLEMENTARY NOTES

19. KEY WORDS (Continue on reverse side if necessary and identify by block number)

Fog Forecasting, Inversion, Marine Fog, Sequential Model
Nearshore Oceanic, California Weather Aircraft Collected Data

20. ABSTRACT (Continue on reverse side if necessary and identify by block number)

Aircraft measurements made offshore during a coastal fog sequence by R.A. Markson are analyzed. Fog occurrence and areal extent are determined using aircraft, ship and shore station observations obtained during the Cooperative Experiment in West Coast Oceanography and Meteorology--1976 along with analyzed satellite visual and infra-red imagery. The offshore conditions are compared with those at the shore stations using

selected fog indices. Photographs of special features observed
are included.

The offshore conditions are classified into phases by
assigning limits within the specified fog indices used in the
modified Leipper fog model. The sequence of observed fog
events is compared to the ideal sequence. The trends in the
sequence are analyzed and a general relationship between the
phase sequence and the local offshore flow is indicated. The
Leipper indices, the San Diego raob and the sequential fog
model appear to be useful in fog prediction for the nearshore
oceanic region from San Diego to Point Conception.

Santa Ana Associated Offshore Fog:
Forecasting With A Sequential Model

by

Douglas Allen Backes
Lieutenant, United States Navy
B.S. United States Naval Academy, 1970

Submitted in partial fulfillment of the
requirements for the degree of

MASTER OF SCIENCE IN OCEANOGRAPHY

from the
NAVAL POSTGRADUATE SCHOOL
September 1977

NAVAL POSTGRADUATE SCHOOL
Monterey, California

Rear Admiral Isham Linder   Jack R. Borsting
Superintendent   Provost

Reproduction of all or part of this report is authorized.

Released as a
Technical Report by:

NAVAL POSTGRADUATE SCHOOL
Monterey, California

Rear Admiral Isham Linder   Jack R. Borsting
Superintendent   Provost

Reproduction of all or part of this report is authorized.

Released as a
Technical Report by:

ABSTRACT

Aircraft measurements made offshore during a coastal
fog sequence by R.A. Markson are analyzed. Fog occurrence
and areal extent are determined using aircraft, ship and
shore station observations obtained during the Cooperative
Experiment in West Coast Oceanography and Meteorology--1976
along with analyzed satellite visual and infra-red imagery.
The offshore conditions are compared with those at the shore
stations using selected fog indices. Photographs of special
features observed are included.

The offshore conditions are classified into phases by
assigning limits within the specified fog indices used in
the modified Leipper fog model. The sequence of observed
fog events is compared to the ideal sequence. The trends
in the sequence are analyzed and a general relationship
between the phase sequence and the local offshore flow is
indicated. The Leipper indices, the San Diego raob and
the sequential fog model appear to be useful in fog prediction
for the nearshore oceanic region from San Diego to Point
Conception.

TABLE OF CONTENTS

LIST OF TABLES

8

LIST OF ILLUSTRATIONS

TABLE OF SYMBOLS AND ABBREVIATIONS

ALT	Altitude
BI	Height of the Base of the Temperature Inversion
CEWCOM '76	Cooperative Experiment in West Coast Oceanography and Meteorology--1976 (Naval Postgraduate School and Naval Ocean Systems Center)
Cu	Cumulus cloud
C	Temperature in degrees Celcius
DMSP	Defense Meteorological Satellite Programme
m	Meters
MI	Moisture Index
M_3	Mixing Ratio at 3000 m
PDT	Pacific Daylight Time
Pt.M	Point Mugu
raob	Radiosonde observation
SAN	San Diego
SCI	San Clemente Island
SNI	San Nicolas Island
St	Stratus cloud
Std Dev	Standard deviation
T	Temperature
T_s	Sea Surface Temperature
T_t	Temperature at the Top of the Temperature Inversion
TI	Temperature Index
$\ominus$	Potential Temperature
$\oplus$	Scattered clouds
	Broken clouds
$\oplus$	Overcast clouds

ACKNOWLEDGEMENT

I. INTRODUCTION

The study of marine fog along the Southern California coast has received attention for many years. This is understandable considering the well-documented hazard imposed by marine fog on coastal shipping and air traffic and the number and importance of military bases there. The prediction of marine fog in the nearshore area is fast becoming a major problem as shipping traffic even now increases with the arrival of Alaskan north slope oil at the California refineries.

Fog forecasting has been one of the most difficult tasks the local forecaster has had to deal with. He must in effect forecast the occurrence of a particular type of cloud, its vertical dimensions, the visibility within the cloud, the time of its onset along with its duration and areal extent. It is even more difficult along the coast where there is almost a complete lack of data upwind of the station. Leipper (1948) describes a method of marine fog forecasting at San Diego using a model evaluated by simple non-diurnal indices. The indices are derived at the station using the radiosonde observations and the sea surface temperature near the station. The method has enjoyed some success at the station but the forecaster using it could only speculate on conditions in the nearshore region off the coast. The problem has been a lack of information as to what was occurring offshore during the progress of the coastal fog sequence.

CEWCOM '76 (Cooperative Experiment in West Coast
Oceanography and Meteorology--1976) provided a unique
opportunity to determine what was actually occurring off-
shore during a real sequence of fog events and to test those
speculations of offshore processes and the areal extent for
which these indices are effective. Aircraft studies of the
offshore atmosphere have been conducted in the past but
mainly have been concerned with the nature of the inversion
capping the marine layer (Edinger 1971). The emphasis was
not on the fog problem and specific features found offshore
were not linked to the onshore fog situation. The present
study examines aircraft vertical soundings of temperature
with altitude and related observations of sea surface
temperature to help answer the question of what happens
offshore as fog occurs at shore stations. Aircraft
observations will be combined with DMSP (Defense Meteor-
logical Satellite Program) visual and infra-red imagery of
the oceanic regime just off the southern California coast.
With shore and ship observations used as "ground truth",
the resulting areal depiction will show offshore conditions
during the fog events. The offshore condition will then be
compared to the shore measurements in light of common
Leipper indices and the sequential fog model (Beardsley
1976).

II.   OBJECTIVES

A.   To utilize aircraft data collected during CEWCOM '76
in order to obtain a comprehensive description of off-
shore conditions present during the Santa Ana fog
sequence from 3 to 12 October 1976.

B.   To compare these findings with conditions as measured at
reporting shore stations by means of fog forecasting
indices.

   1.   Determine the offshore areal extent for which the
indices depict the fog conditions that should be
present.

   2.   Examine factors that affect the Leipper indices with
the objective of forecasting their values.

C.   To define phases of the fog sequence using the height
of the inversion base as the determining parameter and
to compare the actual fog distribution with that ascribed
to the individual phases of an ideal sequence.

III. BACKGROUND

Aircraft meteorological data over coastal waters is made more meaningful by a description of those factors affecting the local marine environment. For example, topographic features along the California coast modify the weather at the various local stations and contribute extensively toward the occurrence and persistence of fog along the coastline. Local effects often modify synoptic scale circulations. Mesoscale oceanographic features may trigger the actual occurrence of fog.

The factors to be examined in this section are:

A. Relief Features

B. Atmospheric Circulation during CEWCOM '76

C. Sea Surface Temperature

D. The Atmospheric Temperature Inversion

A. RELIEF FEATURES

Three major relief features present themselves as contributory to the formation, modification and advection of coastal marine fog. The first examined is the presence of islands off the southern California coastline. These prominences are turbulence forming projections intruding into both the atmospheric and oceanic circulation patterns. Atmospheric eddies and waves are described by Edinger (1971). The effects of islands on the inversion layer seem local; however, larger scale effects such as the lee island fog (Figure C-1) on 10 October can be dramatic. Oceanographically

the islands are part of the second feature, the general
coastal bathymetry. Satellite imagery (Figure B-3)
illustrates the many eddies and anomalous flows present
in the California Current as it flows along the West Coast.
These vagaries, it has been argued, are in part controlled
by the large submarine, island and coastal features of the
area.

The third topographic feature is the coastal range. The
coastal topography is a mixture of low coastal mountains
and intervening valleys, notably the Santa Clara River
Valley and the Los Angeles Basin. The mountains effectively
bar the marine layer from proceeding inland and their sea-
ward downslopes provide the elevation drop which warms and
lowers the relative humidity of the offshore winds from
the north and east (Leipper 1948). With westerly winds
the coastal basins and valleys allow the marine layer to
flow inland keeping its identity for tens of miles inland
until the stability is overcome by heating from below
(Edinger 1963). The modification of the geostrophic flow
by the mountains is complex. Part of the problem in the
present study is to determine whether the air coming into
the area will flow down slope or not.

B. ATMOSPHERIC CIRCULATION DURING CEWCOM '76

Local air flow appears to be an essential element in
determining the onset of a fog sequence. The offshore
flow either modifies the local atmospheric structure or
moves the marine layer offshore. Therefore, it is desirable

16

to estimate the onset and strength of this flow as it relates to the sequential model.

During the period examined, the general air flow along the coastal area from Pt. Arguello to San Diego was influenced by the positions and intensities of the East Pacific High and the Mexican Thermal Low Pressure systems. On 3 October, the East Pacific High moved northeastward toward the northwest coast of the United States. The Mexican Low moved northwest into northwestern Mexico and southern California. The effects of these movements and the interaction with the daily sea breeze regime are discussed in connection with the daily data. Estimates of geostrophic wind used in the sequential fog model were made graphically using the 1800Z National Weather Service surface pressure analysis and a geostrophic wind scale, both provided by the Meteorology Department at the Naval Postgraduate School. These maps, readily available locally, give the morning flow prior to the aircraft measurements.

Offshore flow crosses from land to sea at the coastline. The coastline in the flight area runs northwest to southeast on a line from 315° true to 135° true. Effectively, off-shore flow is here taken to be an easterly wind from 350° true to 125° true. The surface pressure maps shown in the daily data are from the Environmental Data Service of the National Oceanic and Atmospheric Administration, "daily weather maps," Weekly Series September 27-October 17, 1976

(Figures A-1). They reflect closely the National Weather Service product and were used as illustrations because of ease and clarity in reproduction.

Estimates of the actual surface winds offshore were made by R.A. Markson from the aircraft during CEWCOM '76. As seen in the tabular data (Appendix A), surface winds observed during the afternoon flights were generally from the west-northwest. On two occasions upper air winds (4 October at 1200 meters, 08 October at 2000 meters) were estimated to be easterly at about 20 miles per hours, confirming offshore geostrophic flow above the inversion base on those days.

C. SEA SURFACE TEMPERATURE

The southern California coastal bathymetry greatly influences the sea surface temperature structure. Point Conception is the breakway point for the California current and provides sheltering for the intrusion of warm waters from the south. The eddies and meanders of cold and warm water make the sea surface temperature structure complex in the CEWCOM '76 experiment area. Figure B-1 is the resultant plot of those aircraft sea surface temperatures recorded at the bottom of the atmospheric soundings. Most of the measurements were made at three meters of altitude so the only error would be in calibration of the infra-red sensor. The dashed lines in Figure B-1 show areas where the contours were blended with those from the GOSSTCOMP Sea Surface Temperature Plot provided by NOAA for 12 October 1976

18

(Figure B-2). Although on a scale that provides little
or no detail, the satellite temperatures are readily
available for use in computing the Leipper indices.
Occurrence of patch fog was compared with observed sea
surface isotherms for possible correlation as described
in the observed sequence. The complete physics of fog
formation and its relation to sea surface temperature is
not yet fully understood and will not be addressed in the
data analysis.[1] Any correlations simply will be noted.

D. TEMPERATURE INVERSION

Research into the nature of the marine layer and the
climate it produces along the west coast of the United
States has been carried out for many years. Of particular
interest to the investigators was the nature of the
atmospheric inversion that caps the moist cool marine
layer. Blake (1928) used pilot balloons and aircraft
temperature recordings to sample the air over the San
Diego area. He found the summer climate was dominated by
the marine layer. His investigation of the inversion
concluded that the height of the inversion base was
usually at about 500 meters with the maximum temperature
reached at a height of about 1250 meters. Pilot balloon
records seemed to show the inversion was not the product

---

[1] For some of the most recent theoretical treatment
of this problem see Oliver, et al.(1977).

19

of desert air flowing out over the cool marine layer but part of large scale drift of continental air caused by anticyclones over the Plateau States. Blake also states that ". . . There is one relation, however, between the free-air and surface temperatures that stands out prominently, i.e., marked inversions are almost certain to be followed by fog or low clouds every month of the year."

Measurements taken by Neiburger (1945) at coastal stations and with a tethered balloon from a ship offshore from southern California demonstrated the inversion base height was fairly constant along the coast and sloped upward from the coast both landward and out to sea. He also cites the lowering of the marine layer offshore during the afternoon. Neiburger, Johnson and Chien (1961) pursued the structure of the inversion offshore over the East Pacific and concluded that the summer inversion was maintained by subsidence as air spread outward from the high pressure center over the East Pacific. The upward slope of the inversion away from the coast (about 1:1000) continued as far as Hawaii. There the summer inversion average height was about 2000 meters versus 300 meters average at the coast where they stated that the cold water held it very close to the surface. According to them, this slope was caused by the marine layer being located over warmer and warmer water along a trajectory from California to Hawaii; this increased convection under the inversion

which became less stable and higher. Diurnal variations
were noted at distances up to 500 nautical miles from the
coast. Edinger and Wurtele (1971) using data from two
summers (1966, 1967) produced both analytical and
observational results on the nature of the marine inversion
near the southern California coast. The afternoon inversion
base lowering noted by Neiburger (1961) was verified as
shown in Figure 1. Large variability was found in the
height of the inversion base over the area on any single
day. The averaged inversion heights for the months of
August-September 1966 showed a difference of 200 m between
the highest and lowest points. In the daily observations
clouds were more prevalent in the areas of higher inversion
base. The top of the marine layer was more irregular near
shore and in areas having the highest inversions. When
the overall marine layer was thicker, the top of the
stratus deck was more uniform. Stratus rows lined up
with the surface wind were observed, as were bow-wave-like
features down wind from the offshore islands.

The inversion base has been used as a forecasting aid
to indicate marine fog or stratus conditions. Leipper
(1948) used the height of the inversion base as one of
several indices to predict the likelihood of fog. Beardsley
(1976) used these Leipper indices to describe several fog
phases which were tied to height ranges of the inversion
base. Both found that marine fog did not occur if the
inversion base was above 400 meters. This agrees with the
theoretical work done, for example, by Oliver, et al (1977).

From: Marine Layer over
sea test range by
Edinger, J.G. and
Wurtele, M.G. for
Commander Pacific
Missile Range
1971
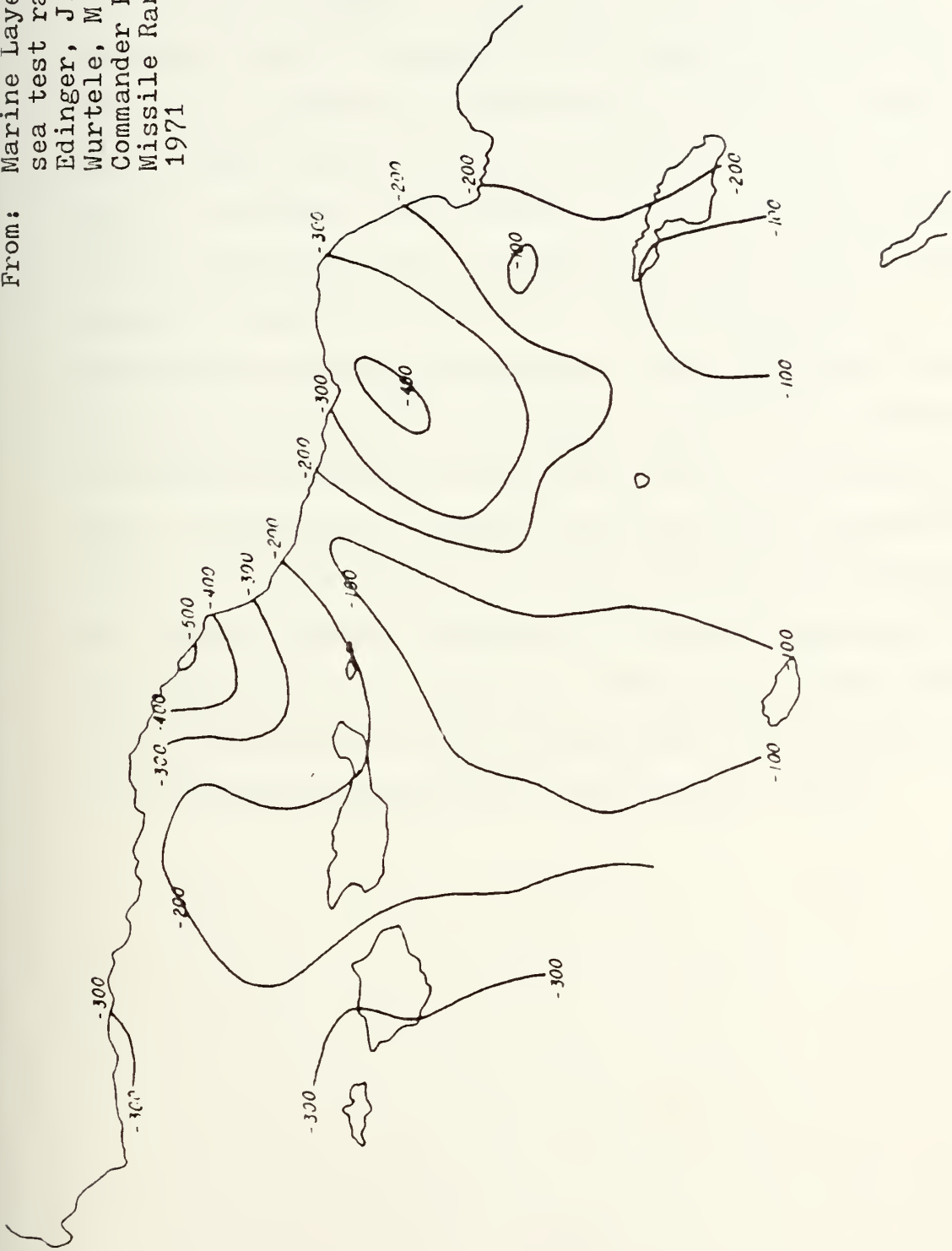
Mean Change in Depth of Marine Layer, Morning to Afternoon, August 1966.

Figure 1

22

Inversion base height measurements have been taken from temperature profiles measured by aircraft soundings offshore during CEWCOM '76. Additional BI (base of the inversion, height) information was taken from shore or ship raobs (radiosonde observations) involved in CEWCOM '76. The aircraft and shore station data are compared with each other to determine the distance to which offshore winds affect the marine layer to seaward. Phases are described using the inversion base as the determining factor. Correlation between inversion base height and local weather is shown to be useful as a forecast guide for the occurrence of marine fog along the California coast. The problem is then to forecast the height of the inversion base near the coast. The model indicates a means to make such predictions by using an expected sequence of inversion height changes and associated fog occurrence. The sequence arises out of the descriptive model which has been tested in selected fog events by Leipper (1948) and Beardsley (1976).

IV. APPROACH

CEWCOM '76 (Cooperative Experiment in West Coast
Oceanography and Meteorology--1976) presented a unique
opportunity to observe the southern California coastal
marine environment. Through the comparison of data
obtained from many platforms including the Research Vessel
Acania, shore facilities at San Diego, San Clemente island,
San Nicolas island and Point Mugu, California, combined
with aircraft and satellite data, a comprehensive picture
of a marine fog event was obtained. The coastal marine
atmospheric environment was closely sampled over the period
from 23 September to 13 October 1976. During that period
a particular sequence of fog occurrences was observed and
monitored. Portions of the many measurements and
observations obtained and analyzed by the author are in
Appendix A, B and C. The reader will be referred to them
in the analysis of the data.

A. SELECTION OF DATA

Although the data were derived from several different
platforms using different measurement techniques and
sensors, they can be made compatible. The careful
combination of these measurements and observations should
contribute toward a comprehensive picture of the atmospheric
conditions during the occurrence of coastal marine fog.

The period from 3 to 12 October was selected for several
reasons. First, it was the period for which aircraft strip

charts were available. The main fog events occurred during that time. Satellite imagery was available for that period also. The flights took place in or near the shore stations' reporting areas, for which the Leipper indices were worked up (White 1977). The ship also operated in the coastal area during this time frame.

B. SOURCES

Radiosonde observations were made at the shore stations three or four times daily except on the weekends when San Clemente island was the only reporting station. Using these raobs and sea surface temperatures from the National Marine Fisheries Service, Bulletin 76-9 (1-15 Oct. 76), the Leipper indices were calculated (White in unpublished work at NPS 1977). The occurrence or non-occurrence of fog was also recorded.

The R/V Acania, operated by the Oceanography Department at the Naval Postgraduate School in Monterey, California, also made radiosonde observations several times daily throughout the period studied. These likewise were analyzed by Lcdr. White.

The aircraft data were collected using a modified Turbo-Bellanca aircraft owned and operated by Dr. Ralph Markson, President of Airborne Research Associates. The data were recorded on an eight channel strip chart recorder mounted in the aircraft. The following parameters were measured:

1. Air temperature (Rosemont probe)
2. Dewpoint (Panametrics aluminum oxide probe)
3. Infra-red sea surface temperature (Barnes PRT-5)
4. C_t^2 (temperature turbulence coefficient)
5. Refractive index of air (NAFI microwave refractometer)
6. Vertical electrical field intensity (radioactive probe)
7. Conductivity (Gerdien tube)
8. Altitude

The four microphysics channels were not used nor was the dewpoint, as the instruement saturated at 10°C and was not usable for determining the offshore MI (Moisture Index). This index required readings up to atmospheric saturation which occurred at temperatures higher than 10°C for the entire period. Air temperature, sea surface temperature and altitude along with pilot commentary containing navigation, visibility and weather phenomena were extracted from the charts. The measured air temperature was calibrated against other air temperature sensors in the aircraft and the Barnes PRT-5 output was compared to ship reported sea temperatures. Comparisons made between the aircraft and ship sea surface temperatures showed the aircraft measurements to be about 0.5°C high when taken near the sea surface. The sea surface temperatures recorded in the daily data tables were measured at the bottom of each aircraft sounding and have not been adjusted. The sea surface temperature plot (Figure B-1) was made using uncorrected aircraft data.

Satellite imagery was used to supplement aircraft visual observations of cloud cover. Blow-ups of the mid-morning DMSP (Defense Meteorlogical Satellite Program) visual and infra-red imagery show the extent of the stratus

and fog in the test area. Shore station, ship, and aircraft observations in the same area provide verification in differentiating fog from low clouds, which is not yet practicable with satellite remote sensing alone. The morning satellite analysis was blended with that from the aircraft observations when practical as shown in the weather depiction of 7, 8, 10 and 11 October when aircraft observational coverage was sufficient. It was shown otherwise as supplemental information on the remaining days of the sequence when aircraft operations were more limited. On 5 October the satellite imagery showed an area of fog between Santa Catalina and San Diego in the morning that had cleared by the time the aircraft sampled the area. This provided the opportunity to identify and measure an area where fog had just dissipated. On 11 October the aircraft soundings H, I, J and K were in an area of active fog formation which the satellite had previously identified as clear of fog or stratus.

The remaining source of data was the National Weather Service 1800Z Surface Pressure analysis for each day of the period. The geostrophic wind was extracted for each day.

C. ARRANGEMENT

The data are located in Appendix A, "Daily Data". This section contains the daily surface pressure analysis with geostrophic wind direction indicated by an arrow over Los Angeles. Appendix A also contains tables of digitized

aircraft soundings for each day (Tables A-II). Each table
is arranged as follows:

    1. Letter designation of each sounding and position.
    2. Time and vertical direction of each sounding.
    3. Air temperature extracted at designated altitude
levels.
    4. The height of the inversion base and minimum
temperature observed at the base.
    5. Potential temperature at the inversion base.
    6. The maximum air temperature at the top of the
inversion and the altitude at which it occurs.
    7. The sea surface temperature recorded at the bottom
of the sounding.
    8. The temperature index for each sounding.
    9. The cloud top and base or, in the absence of
clouds, the top of the haze if present and annotated on
the strip chart.
    10. The surface winds observed from the aircraft.
    11. The average pressure for the area that day taken
from the surface pressure analysis.
    12. Any upper winds recorded.

    The mean values for each day are listed in the second

column from the right. The far right column shows the

standard deviation. This is useful to show variability

of values and at what altitude the soundings were most

variable. The third section of Appendix A is a summary

of all soundings made by aircraft, plus ship and shore

station raobs closest to 1600Z PDT for each day. The

aircraft-derived sea surface temperatures are indicated

by arrows under the aircraft soundings.

    Additional data are displayed on the daily Indices

and Weather Depiction maps (Figures A-4, Appendix A).

Aircraft sounding positions, letter designator, time, BI,

TI, T_s, and wind estimates are shown. Leipper indices

and the occurrence or non-occurrence of fog are located

in designated blocks for each shore station and at the

28

Research Vessel Acania. The remaining features on the maps
are the aircraft and satellite fog observation analyses.

Appendix B contains the sea surface temperature analyses
and Appendix C contains all additional data including
sample photographs of fog and haze taken by Markson in
flight, sample satellite imagery and a photo of the
aircraft.

D. TREATMENT OF AIRCRAFT DATA

Originally three of the measured parameters were to be
analyzed: air temperature and dewpoint versus altitude
and sea surface temperature. These would be comparable
to shore measurements. For reasons previously noted, dew-
point was dropped from the analysis. Sea surface temperature
and altitude were annotated on the strip chart and were
read directly. The air temperature required hand analysis.
A temperature scale was made, using calibration marks and
independent outside air temperature readings, and used to
analyze the pen line recording. This required frequent
recalibration of the scale as the calibration of the
recording device was quite variable. Accuracy of the
temperature readings is estimated to be $\pm0.2°C$.

Vertical soundings made by the aircraft were identified,
positions determined and time noted. The variation of air
temperature versus altitude was graphed for each sounding.
The analysis was restricted to vertical soundings for
several reasons including difficulty in extracting the
data, limited navigational fixing, and length of chart

records (40 to 50 feet per flight). Also, the objectives

of the investigation favored vertical profiles for

comparison to shore stations. Positions of the soundings

are believed accurate to within two to three miles.

Because of the lack of dewpoint measurements the Moisture

Index and the Mixing Ratio were not calculated for the

aircraft soundings. The soundings for each day are

presented in Figures A-3 (a-j) along with shore and ship

raobs near the same time. Tabulated soundings and some of

the flight commentary statistics, shown in Tables A-II (a-j),

were used to describe the weather present on each day as

shown in Figures A-4 (a-j).

The National Weather Service surface pressure analysis

was analyzed for the geostrophic wind over the area.

Frictional effects were not included in the analysis in

order to examine the initial forcing element in offshore

flow. Resistance factors such as friction, opposing sea

breeze and topography do have modifying effects that are

important as to the resultant flow, but these are beyond

the scope of the investigation. The geostrophic flow is

indicated on Figures A-1 (a-j). The aircraft observational

data were used to verify the offshore flow. Aircraft

visual observations were used also as verification of

satellite imagery; first as to the location of clouds,

then as to their nature: high clouds, stratus or fog.

In order to analyze the aircraft soundings within the

context of a trend model such as proposed by Leipper (1948),

the individual soundings were averaged for each day. This

provides a mean off-coast condition which is convenient

as the model treats each day as a whole segment. The time

of this average is taken as the mid-time between the first

and last measurement of the day. The averaged sounding

then can be compared with any shore raobs available on that

day.

V. DATA ANALYSIS

The analysis of the data is done in five stages: First the data are reduced and presented in forms amicable to examining both trends and specific features found in the nearshore regime (Appendix A, B and C). Second, the coastal sequential fog model, adapted for the nearshore region using the aircraft data, is presented. The observed fog sequence then is presented, day-by-day, focusing on those factors or indices thought important to the progress of each phase of the fog event. Frequent references are made to graphical depictions in Appendix A. The day-by-day descriptions are followed by a graphical recap (Figure 2). The observed trends then are summarized.

The fourth stage is to compare the offshore Leipper indices to those recorded at the two coastal stations, Point Mugu and San Diego. This is done in order to determine if indices derived at shore stations can be used to describe offshore conditions. Finally, offshore variability is examined to indicate the offshore areal extent for which the indices may be usable. One additional analysis is made to evaluate the use of the cloud or haze top as an indicator of the height of the inversion base. This method of BI identification has been used in previous aircraft studies of the temperature inversion along the California coast.

A. THE SEQUENTIAL FOG MODEL

It was decided early in the analysis of the aircraft data that common parameters must be used to compare the offshore measurements with those observed from shore stations. The shore stations had been evaluated for fog indices and fog occurrence by White (1977), and that analysis was available to the author. It was decided to attempt a similar scheme whereby different types of fog days might be identified by use of some parametric relation that would define limits distinguishing one day from another. The indices used by Leipper (1948) and applied by Beardsley (1976) in a sequential fog model were assumed to be a good first approximation of daily conditions. The geostrophic wind was added later for trend analysis. It also had some application in the daily data. For the convenience of the reader, the sequential model and the fog forecasting indices may be summarized as follows:

1. The Ideal Fog Sequence

Beardsley (1976) describes an ideal Summer Fog Sequence for use on the Monterey Peninsula using measurements at local sites and the Oakland 0400 (local time) radiosonde. That sequence was derived from the southern California model described by Leipper (1948). His fog model development there was based on shore station observations of winter fog sequences over a three-year period.

Prior to the start of an ideal fog sequence, the East Pacific High moves northeast and inland from its

normal offshore position. This changes the orientation of the surface isobars so as to make them roughly perpendicular to the southern California coast. The anticyclonic circulation about the high brings dry continental air downslope from the inland plateau. It is heated adiabatically and flows offshore warm and dry. This assures the formation of a low inversion.

Phase one conditions expected to be encountered along the coast show the displacement of the marine layer and low level warming with no inversion yet developed. The weather should be clear with light or no sea breeze.

During phase two, the offshore flow has moved the marine layer well offshore, and a heated air column with a surface inversion will be seen in the local morning soundings. There may be some low haze or isolated fog (most likely formed over cold water) but generally clear conditions prevail.

Phase three is defined as follows: The height of the inversion base lies between the sea surface and 150 meters elevation. The East Pacific High beings to retreat to its normal offshore position and the offshore flow decreases. Returning northwesterly surface winds lower the surface air temperature and consequently strengthen the inversion. Fog becomes patchy, occurring where inversion height is greater and over cold water. The marine layer thickens, partly because of radiation cooling from its top. The TI* has stabilized and the MI* increases as the

* defined on the following pages

marine layer becomes more saturated. Fog may clear over most areas during the day leaving haze present, but the fog returns at night.

Phase four (inversion base from 150 to 400 meters in height) is typified by general cooling of the air column above the marine layer. The TI decreases. North-westerlies freshen and fog becomes thicker, covers larger areas and becomes persistent, extending farther inland at night. Low stratus is evident during the afternoon.

With phase five the sequence is concluded as fog does not occur with the high inversion (greater than 400 meters)[2]. The TI decreases to pre-sequence values as the East Pacific High returns to its normal offshore position precluding offshore flow. The upper air continues to cool as the inversion increases in height and decreases in strength.

The sequence may stop at any phase or even reverse, depending on the strength of the offshore flow. When the offshore flow stops the sequence will progress to conclusion. The fifth phase may continue for some time as the persistent stratus common in the summer along the California coast.

Important in the present connection is the fact that no offshore data suitable for use were available when the ideal fog sequence and forecasting indices were developed.

---

[2]This was deduced observationally by Leipper (1948) and is consistent with the latest theoretical work (Oliver et al. 1977).

2. Indices

The indices for the Leipper fog model are used to
aid in the analysis of the CEWCOM '76 aircraft data during
the period from 3 October to 12 October 1976. They are
summarized below:

BI - Height of the Base of the Inversion, measured
above mean sea level in the early morning raob. A BI less
than 400 meters is favorable for fog; a greater BI indicates
a stratus condition. If no inversion is present fog or
stratus is not likely.

TI - Temperature Index: a measure of the presence
of warm Santa Ana flow over the coastal waters. A positive
value is favorable. A high value is indicative of a
potentially strong inversion. $TI = T_t - T_s$, where T_t is
the morning air temperature at top of the inversion and T_s
is the sea surface temperature closest to the reporting
station. Units are $°C$.

MI - Moisture Index: a measure of the relative
amount of moisture in the marine layer during the maximum
sea breeze. $MI = T_{d(0030z)} - T_s$ (on the previous fog day.)
Any value greater than $(-5°C)$ is considered favorable.

M_3 - Mixing Ratio: a measure of the moisture content
of the upper air. It is an indication of the effectiveness
of radiation cooling at the top of the marine layer.
Measured at 3000 meters from the morning raob, a value of
3.5 grams per kilogram or less is favorable for fog development.

These indices can be used as a measure of the
progress of the fog sequence, the relative probabilities
of fog occurrence, and areal extent of the fog formations.
The aircraft dervied indices cited were calculated using
insitu aircraft measurements and were not restricted to
the time constraints of the formal Leipper indices at the
shore stations.

B.   THE OBSERVED FOG SEQUENCE

The observed fog sequence is now reviewed day by day
for the period 3-12 October 1976. On 3 October the fog
sequence was initiated by the East Pacific High moving to
a position 500 miles off the Oregon Coast. The geostrophic
wind over the CEWCOM area was 020°T at 12 knots (Figure A-1-a).
No inversion was detected either offshore or onshore in
the afternoon (Figure A-1-c). The Temperature Index
offshore was zero. No fog was reported along the coast.
A stratus deck was located west of San Clemente Island,
advancing shoreward with the sea breeze by late afternoon
(Figure A-4-a). Phase one conditions prevailed both off-
shore and along the coast.

Phase two was expected for 4 October. High pressure
had extended over the State of Washington; however,
advancing low pressure from Mexico led to geostrophic
flow from 350°T at 10 knots (Figure A-1-b). Aircraft
observed winds at 1200 meters were estimated to be easterly
at 25 knots. The inversion base at 75 meters signalled

37

phase three conditions had already begun. The average offshore temperature index was +4.3°C while San Diego had an inversion at 173 meters with a temperature index of +1.5°C. The moisture index has risen from -5.5°C on 3 October to -2.4°C on 4 October. Warming throughout the air column had occurred at all stations through it was greater in the northeastern sector. There was extreme variability in the inversion base offshore from zero to 250 meters with stratus occurring in the area of maximum inversion height at soundings E and F, shown in Figure A-3-b. Fog occurred only at Point Mugu while offshore the stratus deck retreated to the southwest.

On 5 October the geostrophic flow remained about northerly with a decrease to about 7 knots. The inversion height was uniform offshore averaging about 155 meters. The temperature at the top of the inversion had risen to about 28 C with warming greater to the north. The inversion was noticably lower offshore than at the coast as shown in Figure A-3-c. Sounding C, made at the edge of the advancing stratus, showed the inversion base higher than in the clear areas. Fog was observed at San Diego and Point Mugu along the coast and offshore at San Nicolas Island. The San Nicolas Island fog appears to be associated with the eastern edge of the stratus deck (Figure A-4-c).

Phase four conditions were present both on and offshore on 6 October. The high pressure remained north over southwest Canada with a ridge extending offshore to the

southwest. Offshore flow in the CEWCOM area remained
northerly and weak. The inversion base increased to 235
meters offshore while the temperature at the top of the
inversion remained about 28°C. Stratus spread over the
offshore area where offshore flow moved southerly from
land but it was clear west of Point Arguello (Figure A-4-d).
Fog occurred only at Point Mugu where the inversion base
was lowest on the morning raob. The temperature at the
base of the inversion had dropped steadily since the start
of the sequence.

On 7 October offshore flow from the north ceased as
the East Pacific high pressure was split by a low forming
off Oregon. There is some indication of offshore flow
from the east in the CEWCOM area but it is very light
(Figure A-1-e). The inversion base lowered to an average
of 133 meters in the aircraft soundings which is reflected
on the afternoon raob from Point Mugu. The remaining shore
station BI remained above 200 meters. Phase four existed
onshore with Phase three indicated offshore. This is a
possible artifact of a large afternoon effect. Warming
had continued at the top of the inversion with the average
temperature being 29.0°C. Point Mugu also reflects this
warming (Figure A-3-e). Fog occurred at Point Mugu and
San Nicolas Island and offshore at the edge of the stratus
off Point Conception and at San Nicolas Island. The
temperature at the base of the inversion was low, 18.2°C,
(Figure A-3-e) under the effect of a strong sea breeze from
320°T at 20 knots measured off Point Arguello.

On 8 October, offshore flow increased to about 10 knots and shifted to the east under the influence of the Mexican thermal low pressure system (Figure A-1-f). This easterly flow was estimated at 2000 meters to be 20 knots by the pilot of the aircraft. A high pressure ridge extended from over Idaho to 600 miles off southern California. The inversion base lowered and left patchy fog as the offshore flow shifted to the east. The progress of the lowering seems to follow the geostrophic wind component as the fog and stratus retreated to the west and remained off Point Conception over the cold water (Figure A-4-f). This is reflected in the difference in aircraft soundings (A through F reflect a surface inversion while G through K show elevated inversions). The temperature at the top of the inversion increased to an average of 29.5°C which is reflected also in the Point Mugu and San Diego raobs (Figure A-3-f). Thus, the sequence has shown a definite reversal associated with the revival of stronger offshore flow.

Dawn on 9 October was clear and calm. Offshore flow was from the east to northeast. Along shore the marine layer has been replaced by dry continental air though clouds existed some 100 miles or so offshore. A surface inversion existed in all aircraft soundings with a shallow haze layer offshore of San Diego (Figure A-4-g). Phase two conditions are observed offshore and along the coast. The temperature at the top of the inversion was 31°C, indicating Santa Ana

conditions. The Acania raob was considerably different from all others as it was taken at a position to the northwest of the experiment area and reflects the returning marine layer farther offshore. Phase three is expected for 10 October.

Geostrophic flow returned to the north on 10 October but remained light. The inversion had increased to an average of 115 meters offshore. San Clemente Island, the only reporting shore station, had a weak inversion at 150 meters (Figure A-3-h). The inversion height was fairly consistent throughout the area with the temperature at the top of the inversion falling to an average of 27.5°C. Fog was located in large patches along the coast with the stratus deck offshore southwest of San Clemente Island. There was a clear area between the deck and the coastal fog. The Moisture Index onshore had increased from -6.7°C on 8 October to -5.6°C at Point Mugu, the only station reporting fog. In this case the offshore fog was much more extensive than indicated by phase three conditions, occurring almost all along the coastline but generally just slightly offshore (Figure A-4-h). Of particular interest was the lee island effects observed by Markson downwind of Santa Catalina Island (Figure C-1). Fog persisted behind the island during the entire flight. As phase three was expected and observed, the ideal sequence pattern seems to have resumed.

The inversion on 11 October increased to an average of 275 meters with cooling at both the top to 24.3°C and at the base to 18.5°C. Geostrophic flow continued from the north; however, the East Pacific high pressure had moved north extending toward the Oregon coast. San Clemente reported an inversion base at 350 meters on the afternoon raob while the R/V Acania had a 370 meter inversion (Figure A-3-i). Fog was reported at three of the four shore stations, consistent with <u>phase</u> <u>four</u> conditions. Fog was observed reforming in the late afternoon in the area of soundings H through K (Figure A-4-i).

On 12 October the aircraft remained close to San Diego and wide area coverage was not possible. Satellite imagery showed a general coverage of the area with stratus and fog. The inversion base continued to increase in height to an average of 365 meters offshore though the Point Mugu raob shows the inversion decreasing to 250 meters. Geostrophic flow was from the northeast at 10 knots as a high pressure ridge was formed from Washington to a position 800 miles off southern California (Figure A-1-j). Offshore flow also was indicated in the warming at the top of the inversion to 27.9°C in the aircraft soundings and to 30°C at Point Mugu. Again, Point Mugu leads the southern area in the appearance of offshore flow. The 12th of October was the final day of aircraft data.

C.   TREND SUMMARY

Figure 2 gives a graphical summary of the aircraft observations throughout the fog sequence. The influx of warm continental air over the coastal waters can be seen in the progression of the average aircraft soundings for each day of the sequence. As the warm air moves over the water the inversion forms by 4 October and lifts and strengthens on 5 through 7 October, with the concurrent formation of fog. The fog sequence progresses through phase four until 7 October when increased offshore flow reverses the sequence back to phase two which is reached on 9 October. The flow diminishes and shifts to the north on 10 October and the sequence resumes normal progression to phase four/five on 12 October. Examination of the TI and the offshore normal component of the geostrophic flow reveals a controlling affect on the BI. As the ideal sequence suggests, fog occurrence may be predicted to vary with each phase. The maximum fog coverage did in fact occur on phase four days as shown in the fog occurrence figures at the bottom of the summary. Comparison of days of similar phase shows similar offshore situations as seen by examining the Daily Indices and Weather Depiction maps in Appendix A. Phase two conditions on 9 October are very different from phase four conditions as seen by comparing 6 to 9 October. Conversely, the situations on 6 and 11 October represent the same phase and are quite similar.

43

Averaged Aircraft Soundings,   3 - 12 October 1976

Alt. (m)

1200

800

400

sfc

3   4   5   6   7   8   9   10   11   12

15° 20°   20   20   20   20   20   20   20   20   20°

Temperature (°C)
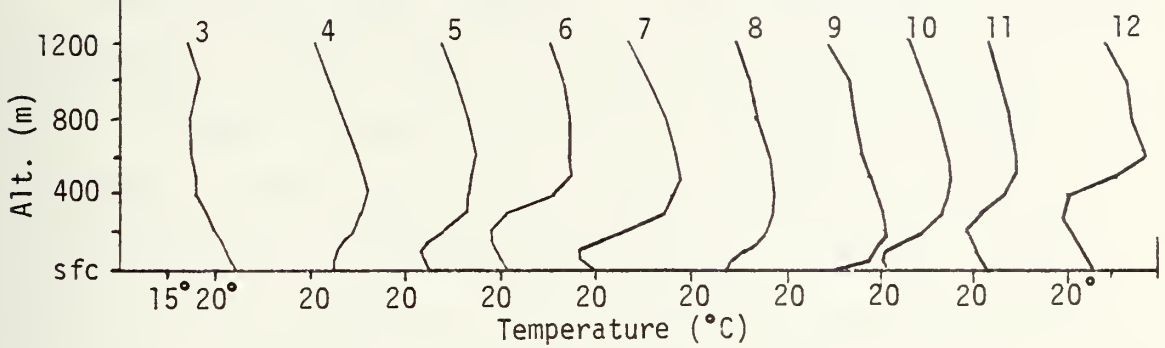
NO. of observations per day:

| 3 | 6 | 7 | 5 | 10 | 11 | 7 | 18 | 10 | 3 |

Time span of aircraft soundings:

| 1638 | 1628 | 1412 | 1504 | 1415 | 1300 | 1107 | 1309 | 1443 | 1516 |
| 1842 | 1850 | 1630 | 1710 | 1819 | 1809 | 1240 | 1809 | 1759 | 1552 |

date:	3	4	5	6	7	8	9	10	11	12
PHASE:	1	3	3/4	4	3	2/3	2	3	4	4/5

Aircraft parameters:

Alt. (m)

600

400

200

sfc

TI

BI

TI (°C)

+10

+5

0

-5

Date: 3   4   5   6   7   8   9   10   11   12

Strength of normal component of offshore flow (geostrophic)

Vel. (nm/hr)

30
20
10
0

Date: 3   4   5   6   7   8   9   10   11   12
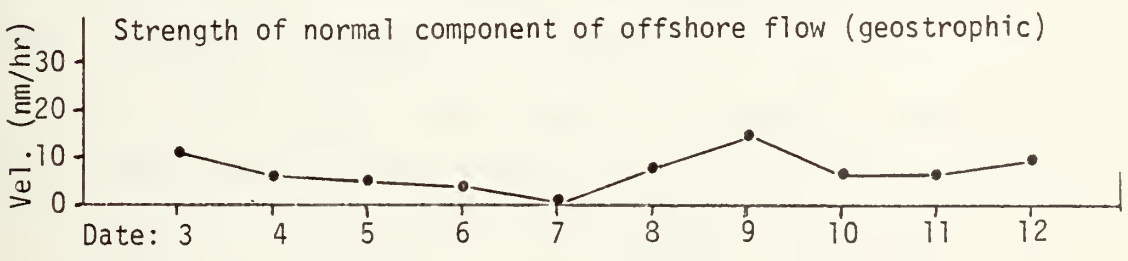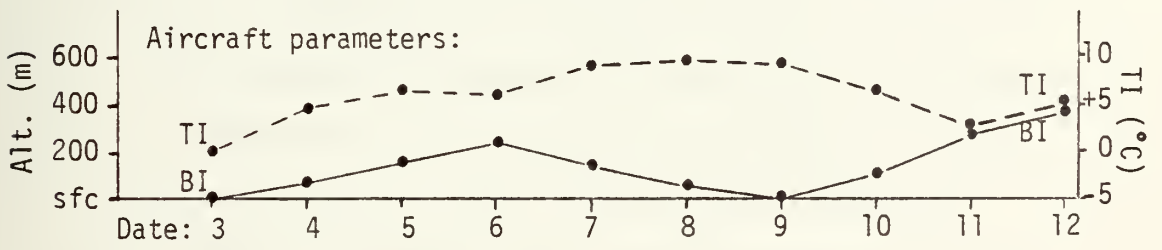
Fog occurrence; (No. of sources reporting fog) (Max. on-4,off-3)

| Onshore | 0 | 1 | 3 | 2 | 2 | 1 | 0 | 1 | 3 | 1 |
| Offshore | 0 | 0 | 2 | 1 | 1 | 2 | 1 | 3 | 2 | 1 |

Figure 2.   Analysis Summary: The Fog Sequence   3-12 Oct 76

D. COMPARISON OF SHORE STATION DATA TO AIRCRAFT DATA

The BI and TI were chosen to compare shore and aircraft observations as they were the available indices at both sites. Figure 3 shows a plot of the inversion height measured at Point Mugu and San Diego during the morning raob versus the averaged aircraft BI for each day. The purpose is to determine if the relative changes in each are alike, showing a common trend. The shore stations did not make radiosonde observations on 3, 9, 10 and 11 October; however, there are enough common days to make a comparison. Examining the graph day-by-day for discrepancies between aircraft and shore immediately shows a mismatch between the aircraft and Point Mugu on 4 October. The effect can be explained by looking at Figure A-3-b and A-4-b. The aircraft averaged BI does not reflect the spatial differences in inversion heights which existed. Just west of Catalina Island the aircraft measured inversion was 250 meters which almost matches the 258 meter inversion measured at Point Mugu.

On 5 October there was a very low inversion base at Point Mugu associated with local fog. However, by 0800 PDT the inversion had returned to 200 meters, comparing favorably to the 155 meter average BI from aircraft observations. The sixth of October showed good correlation; however, on 7 October there was a large variation between offshore and onshore readings. Examination of the shore raobs near the midtime of the aircraft flight showed that
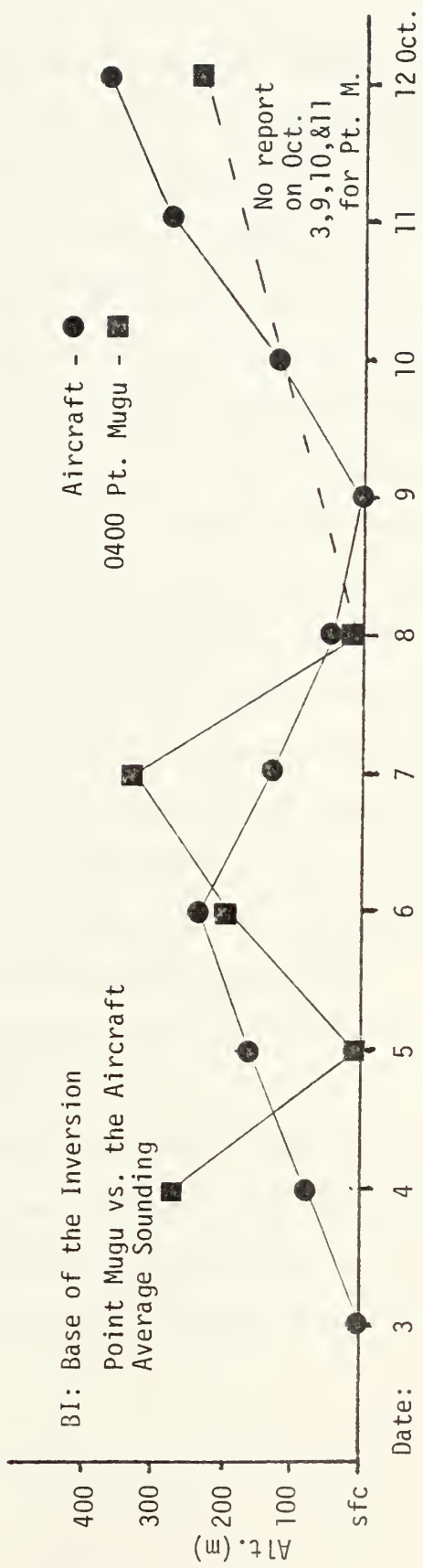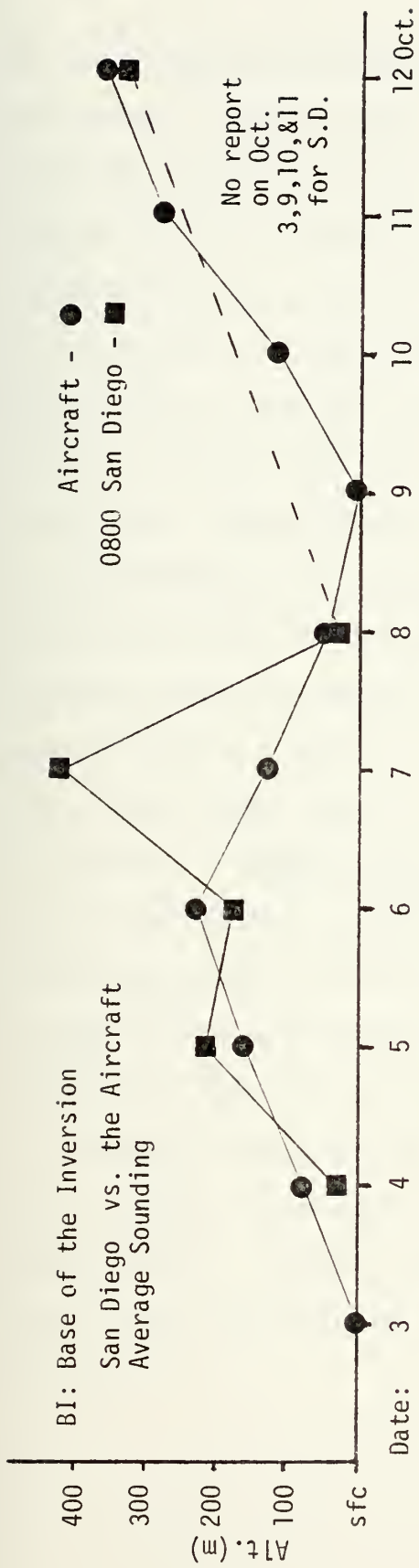
Figure 3. Comparison of BI; Aircraft to Shore

the Point Mugu inversion had dropped from 324 meters to
100 meters, and San Diego from 419 meters to 230 meters,
compared to the 135 meter average recorded by the aircraft
(Figure A-3-e). The difference is a good example of
temporal change in the inversion characteristics caused
by the arrival of warm continental air pushing offshore
during the mid morning. Here the Leipper indices measured
from the morning raob lag the actual situation that is
occurring. Examination of the surface pressure analysis
for geostrophic flow (Figure A-1-e) for the morning does
not yet show the flow starting. The offshore flow had
started between sampling intervals of the model. The
remaining days seemed in phase as the sequence reversals
halted with phase two on 9 October; then the sequence
progressed to phase four/five on 12 October. Other than
some small diurnal effects and the spatial and temporal
variations noted, the BI measured onshore reflected
generally the conditions experienced off the coast as
sampled by aircraft during CEWCOM '76.

Making a similar comparison using the TI shows an
even stronger correlation between offshore and onshore
measurements. Figure 4 shows the comparison of TI as
calculated at San Diego and Point Mugu versus the aircraft
averaged TI.
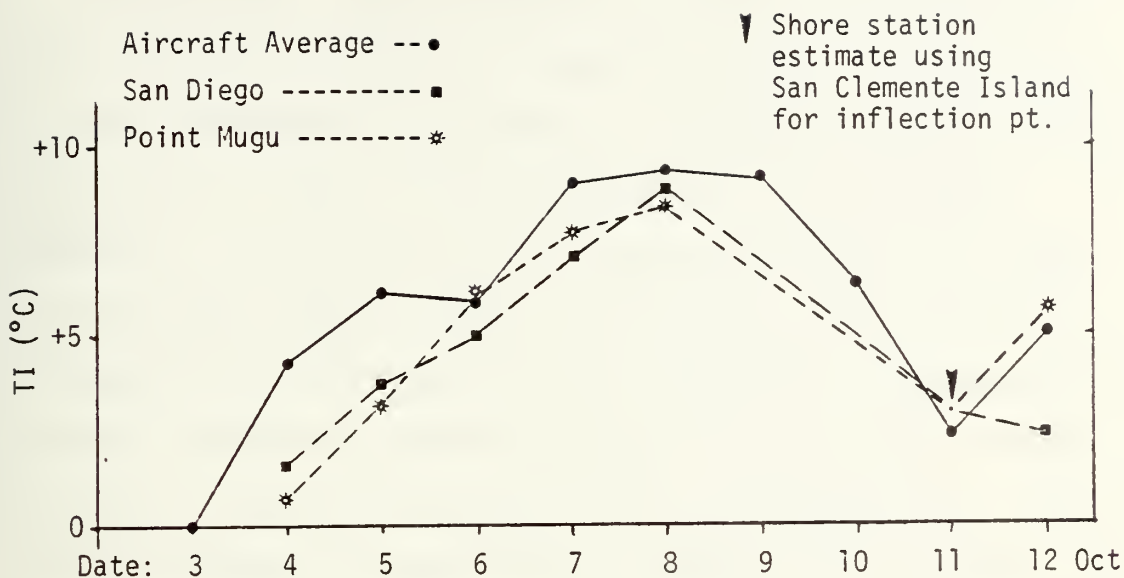
Figure 4. Comparison of TI; Aircraft to Shore

It is apparent that the trends at the shore stations are closely mirrored in the near offshore regime. Thus, predictions of fog occurrence made at San Diego using the fog sequence model are applicable for use in the offshore area. It is now useful to examine the areal extent for which the fog predictions may be usable. The method chosen examines the variability of the BI along and off the coast from the San Diego area.

E.   VARIABILITY OF AIRCRAFT MEASURED INDICES

Variability of the aircraft soundings was considered in two aspects, spatial and temporal. Spatial variability is shown graphically in Figure 5. Using the inversion base as a specific measure of the character of the aircraft sounding, a cross section was constructed along the coast for the three days the aircraft traversed the length of the coast from San Diego to Point Arguello. The graphs for each day shows distance upcoast from San Diego versus altitude at which the inversion base was encountered. The letter designator at each point indicates the sounding used (Tables A-II and Figures A-3 and A-4). The purpose for the analysis was to investigate the areal extent for which the Leipper parameters measured at San Diego might be valid.

October 7, a _phase_ _three_ day (Figure 5), shows a BI maximum difference of 80 meters between any two soundings. The average inversion height is 135 meters. The maximum height occurred off the northwest tip of Catalina Island with the minimum height in the Santa Barbara Channel. Off Point Conception there is a gradual step-up in the BI from clear to fog to stratus sky conditions.

On 8 October the most dramatic spatial variation can be seen off Point Arguello. A surface inversion was present from San Diego to Point Conception with no variability. The offshore region west of Point Arguello appears completely decoupled from the rest of the area. The difference

Variability of the Inversion Base along the coast: (View is cross sectional Looking Toward the Coast)
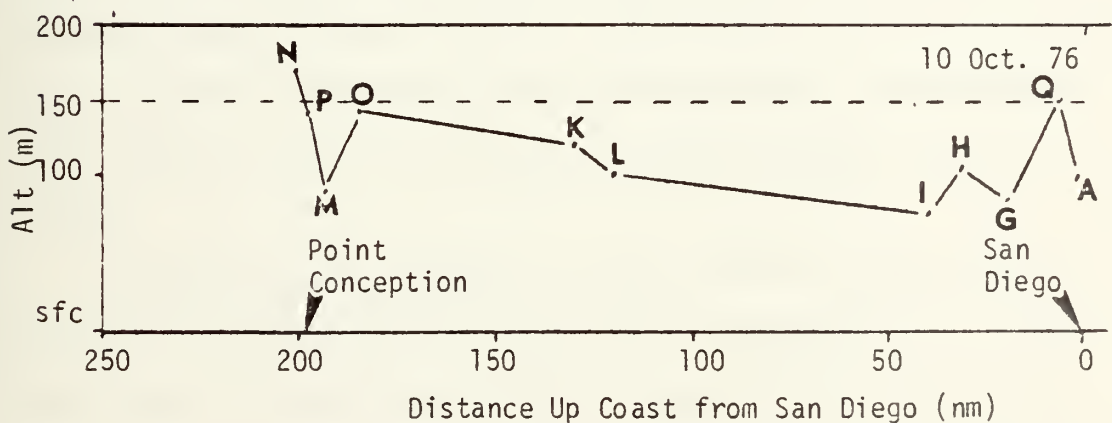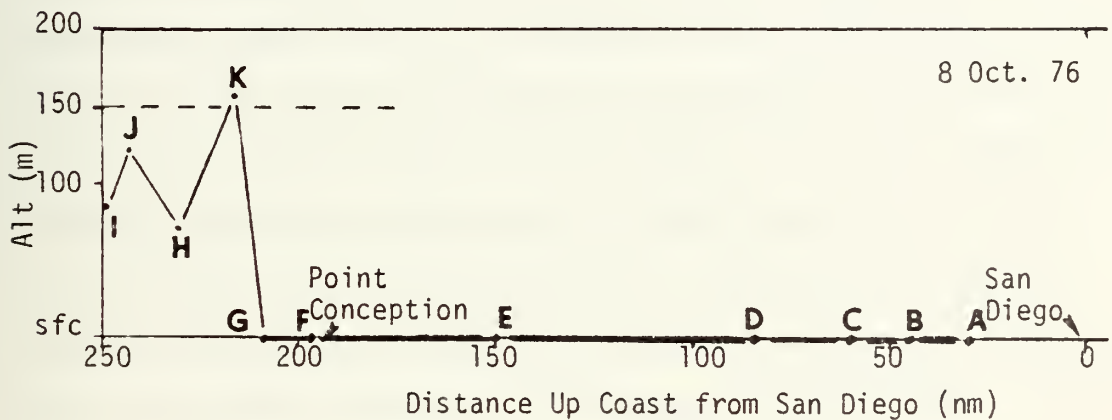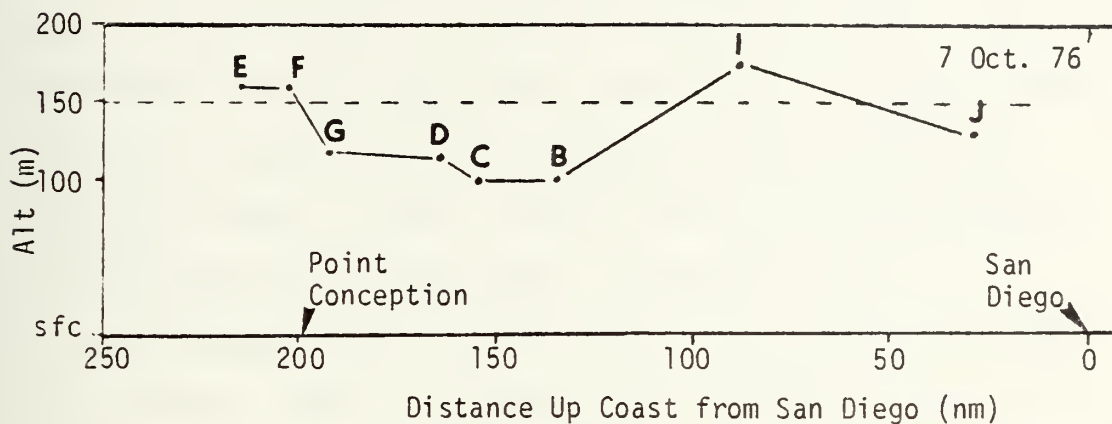
Figure 5. Variability of the Inversion Base

between soundings G and K is 160 meters. The offshore flow present over most of the area has not appreciably affected the area west of a line south from Point Arguello. The temperature at the top of the inversion was 2 to 4°C lower than east of the line and the layer below the BI was 5 to 10°C colder. Heavy fog and stratus further offshore are associated with the higher inversion base.

On 10 October the depiction was very similar to that on 8 October. When cloud cover was compared to the sea surface temperature plots (both aircraft (Figure B-1) and GOSSTCOMP (Figure B-2)), it appeared that the clouds existed over the cold water and where the geostrophic flow was not offshore. Further south the situation was quite different. Offshore flow was experienced at the other fog locations and the water was relatively warm. The fog was located both in the lee of an island northeast of Catalina Island and in the open waters off Point Mugu and San Diego. The BI varied between 90 and 130 meters in the fog patch just off San Diego (Figure A-4-h). The average BI was 115 meters and consistent with the patchy fog present. The maximum difference in the BI between any two soundings was 80 meters.

Comparison of nearshore to far offshore soundings is limited to those times the aircraft ventured close to the consistent stratus deck located from 40 to 120 nautical miles from the coast. This is best seen in the 11 October Indices and Weather Depiction map (Figure A-4-i).

Soundings A and B are in the clear area about 30 miles from shore whereas C and D are near or in the stratus deck about 50 nautical miles from shore. As the aircraft sampled closer to the offshore stratus deck the BI rose from 240 meters at sounding B to 400 meters at the stratus edge in sounding D. This seems consistent with other soundings close to the edge of the offshore deck. It also seems to signal the effective limit to offshore flow lowering the BI and Leipper indices applicability.[3]

Temporal variability was not easily deduced from the aircraft data as the aircraft rarely revisited previous sounding sites on the same flight. The Indices and Weather Depiction maps do show three occasions on which revisits detected temporal change. On 7 October movement of the stratus deck toward shore in the San Diego area was detected over a time difference of four hours. On 10 October changes were noted in the shape of the fog patches off Point Mugu and leeward off Santa Catalina Island. The San Diego area on that day had soundings about five hours apart just offshore. The BI changed from about 100 to 150 meters and a stratus deck was forming offshore from the previous fog patches. On 11 October there was active formation of fog just off La Jolla where only haze existed at the beginning of the flight.

_____

[3] If calculated from the San Diego raob.

Comparison of the top of the haze or clouds to the
height of the inversion base demonstrated another feature
of aircraft sounding variability. It was decided to check
possible correlation by a comparison of the height of the
inversion base to the height of the top of the haze or
clouds (fog or stratus). This correlation was assumed
by Edinger (1971) when the tops of stratus were taken to
be about the same as the height of the inversion base. The
following table records the daily average altitude at the
top of the cloud or haze and the height of the inversion
base if both were recorded during the soundings. The
number of soundings used for the average are shown below
each column in Table I.

Date:	3	4		5		6		7		8	
Haze/Cld. Top (m)	800	350	240	235	260	–	280	155	220	900	40
BI (m)	none	sfc	225	145	205	–	235	155	140	65	sfc
Difference (m)	– –	350	15	90	55	–	45	0	80	835	40
# of obs.	2 0	2	2	5	1	0	5	2	2	7	1

Date:	9	10		11		12		ave dif	
Haze/Cld. Top (m)	clear	115	120	245	440	365	420		
BI (m)	sfc	135	135	260	400	300	400		
Difference (m)	–	-20	-15	-15	40	65	20	186	35
# of obs.	6	7	10	8	1	1	2	32	24

Table I: Cloud Tops vs. BI   3-12 Oct 76

The difference between BI and the tops were calculated
for each day. The sequence average was also calculated.
For haze it was 186 meters based on 32 soundings and for
clouds it was 35 meters based on 24 soundings. After
removing four soundings on 8 October when a light haze
layer was recorded at an altitude of 1500 meters, the
average difference for 8 October reduced to 105 meters.
The overall difference between haze top and BI then became
82 meters.

VI. CONCLUSIONS

From the analysis of the data in Appendix A it has been determined that the near offshore aircraft soundings were similar to the radiosonde observations at San Diego within the confines of the phases of the sequential fog model.

. When the height of the inversion base had a large variation the clouds or fog were generally found in areas of higher bases.

The inversion layer itself can contain haze or clouds above the inversion base and the top of the clouds or haze was not always a true reflection of the height of the base of the inversion.

Satellite imagery provided valuable information on offshore coverage of fog or stratus and was a remote measure of the phase of the sequential model and thus of inversion height.

The offshore flow has a large influence on the inversion height distribution in the souther California coastal area. Whereas strong flow lowers the inversion base or moves the marine layer offshore, cessation of offshore flow permits the inversion base to lift and the marine layer to return.

The sequential fog model using the Leipper indices at San Diego can be a valuable tool in the forecasting of fog offshore along the souther California coast. The model for San Diego was valid for the off coast area from

Point Conception south to the Los Coronados Islands and out to the edge of the stratus deck as determined by satellite imagery.

The speed and direction of the geostrophic flow as determined from the surface pressure analysis was useful in predicting the onset and progression of the Santa Ana fog sequence.

Figure A-1-a'   Surface Pressure Analysis   2 Oct 76
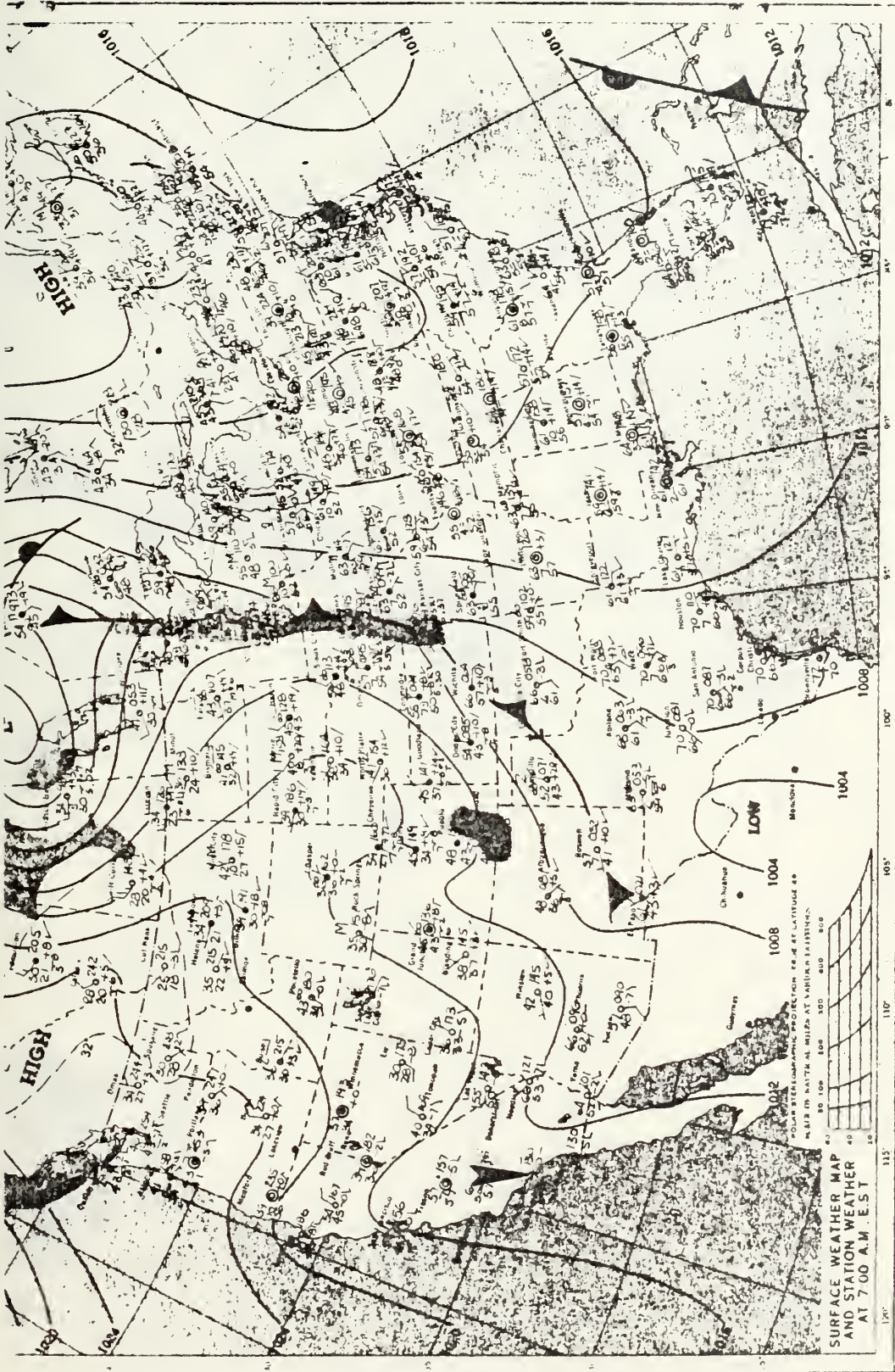
Figure A-1-a   Surface Pressure Analysis   3 Oct 76

Figure A-1-b   Surface Pressure Analysis   4 Oct 76

Figure A-1-c   Surface Pressure Analysis   5 Oct 76
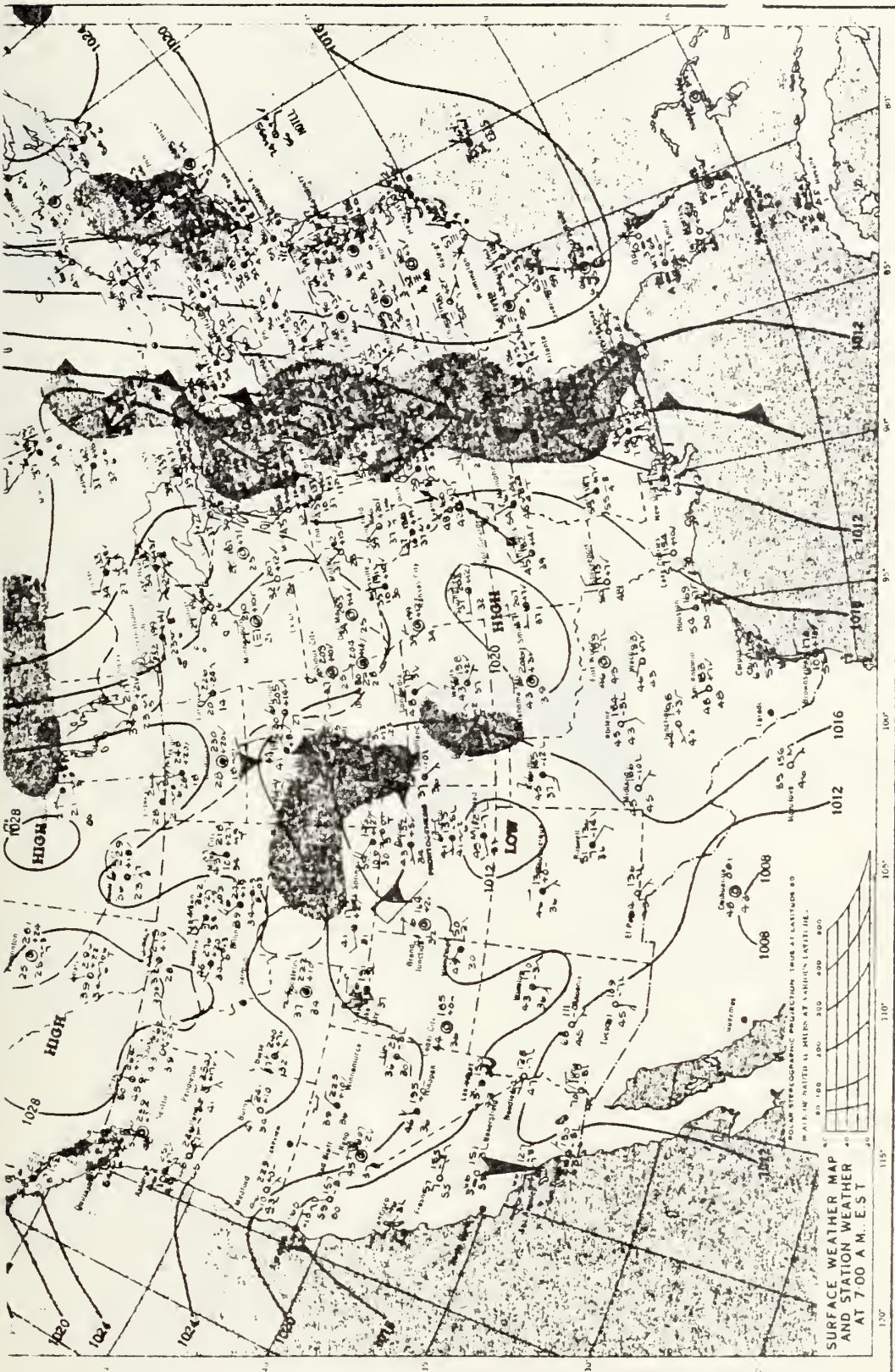
Figure A-1-d   Surface Pressure Analysis

6 Oct 76

Figure A-1-e   Surface Pressure Analysis   7 Oct 76

Figure A-1-f   Surface Pressure Analysis   8 Oct 76
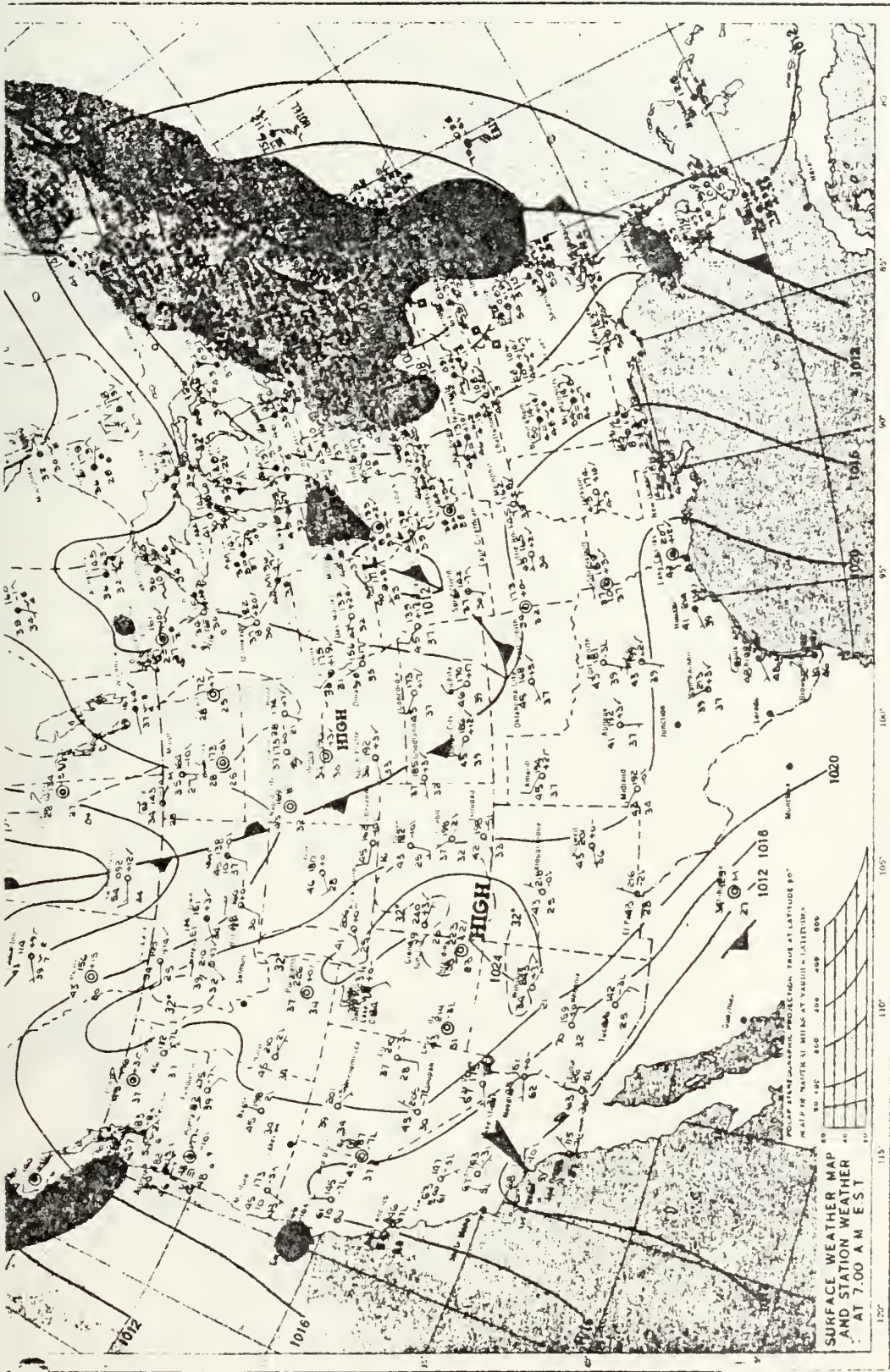
Figure A-1-g   Surface Pressure Analysis   9 Oct 76

Figure A-1-h   Surface Pressure Analysis   10 Oct 76
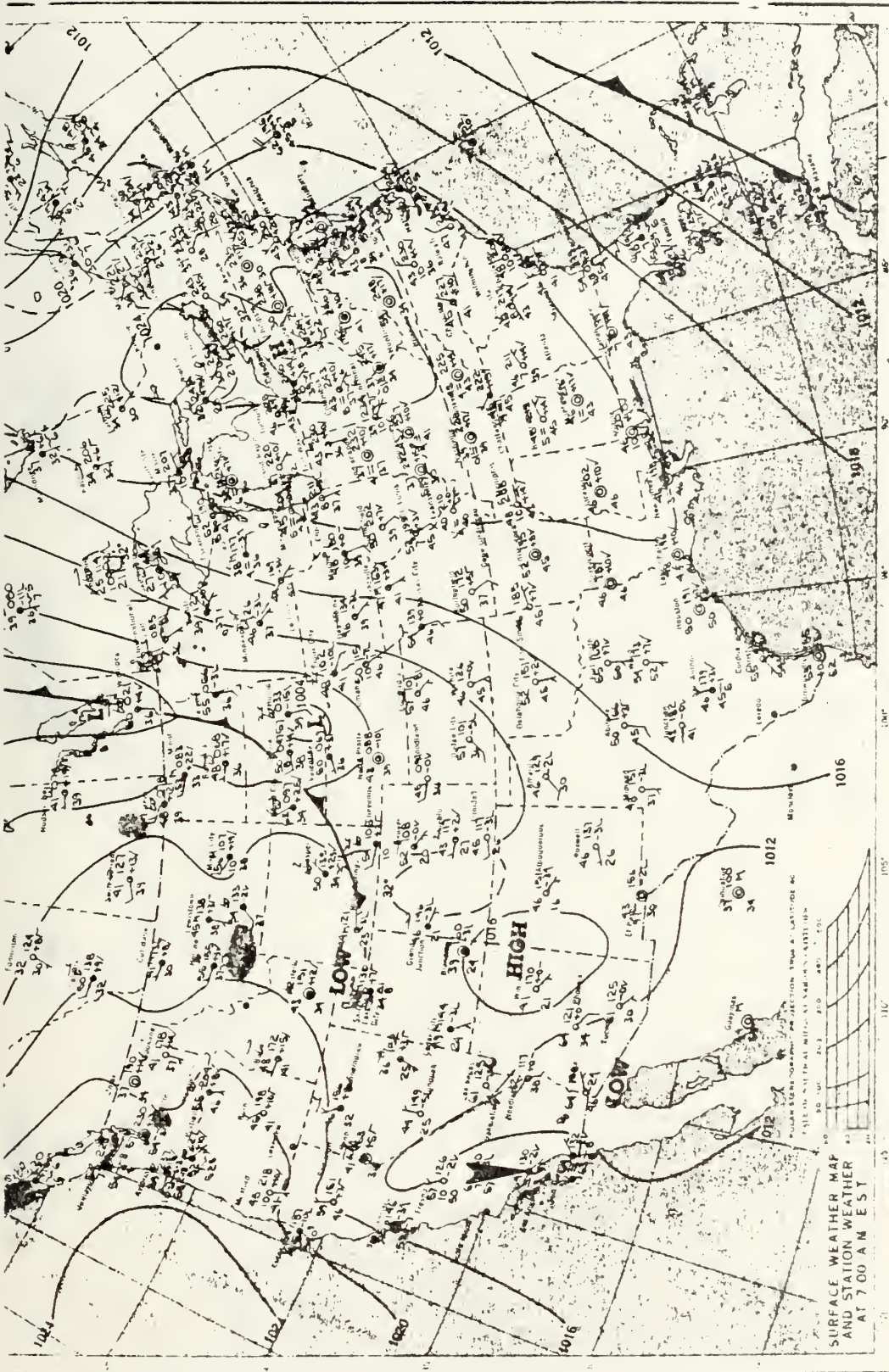
Figure A-1-i   Surface Pressure Analysis   11 Oct 76

Figure A-1-j   Surface Pressure Analysis   12 Oct 76

Sounding	A	B	C	Mean	Std.Dev.
Lat N	32-50	32-49	32-48		
Lon W	117-17	117-18	117-19		
Time PDT	▲ 1638	▼ 1821	▲ 1842	1740	
Alt(m) T(°C)					
(Bottom)	(3) 21.3	(3) 22.3	(30) 22.0	21.9	0.5
50	20.5	21.8	21.8	21.4	0.7
100	20.0	21.2	21.2	20.9	0.8
150	19.8	20.8	20.8	20.5	0.6
200	19.2	20.2	20.4	19.9	0.6
300	18.5	19.0	19.5	19.0	0.5
400	17.5	18.0	18.0	17.8	0.3
500	17.3	18.0		17.7	0.5
600	16.6	17.8		17.2	0.8
800	16.0	18.6		17.3	1.8
1000		18.3		18.3	0.0
1200		17.0		17.0	0.0
(BI)	none	none	none	none	0
θ at BI	N/A	N/A	N/A	N/A	
T_t	sfc 21.3	sfc 22.3	sfc 22.0	sfc 21.7	0/0.5
T_s	21.3	22.5	22.1	22.0	0.6
TI (°C)	+0.0	-0.2	+0.2	+0.0	0.2
Cloud Top(m)	800	800	unk	800	0
Cloud Base(m)	haze	haze	haze	haze	
Surf Wind	250 / 10	270 / 10	270 / 05	265 / 08	011/03

Table A-II-a   Aircraft Data: Daily Digitized Analysis   3 Oct 76

Sounding	A	B	C	D	E	F	G	Mean	Std.Dev.
Lat N	33-15	33-16	33-20	33-17	33-24	33-33	33-20		
Lon W	117-57	118-05	118-11	118-32	119-05	119-00	117-55		
Time PDT	1628	1648	1710	1727	1806	1822	1850	1739	
Alt(m) T(°C)									
(Bottom)	(15) 22.4	(3) 22.0	(3) 24.2	(3) 22.8	(3) 22.0	(6) 22.0	(30) 22.0	22.5	1.3
50	22.5	22.5	25.6	23.0	22.0	22.0	20.0	22.6	1.8
100	23.2	22.5	26.0	24.0	21.2	21.4	20.5	22.9	2.0
150	23.8	23.4	27.2	24.4	21.0	20.5	21.0	23.5	2.3
200	24.8	24.5	28.2	25.4	22.0	19.8	22.2	24.5	2.3
300	25.6	25.7	28.0	25.8	22.6	23.0	24.0	25.3	1.8
400	26.8	26.5	28.0	25.8	25.2	24.0	23.8	26.0	1.4
500	26.8	26.0	27.4	25.4	25.8	24.5	23.4	25.8	1.4
600	26.0	25.8	27.0	24.0	25.4	24.0	22.5	25.1	1.4
800	unk	24.2	24.8	22.8	24.0	22.8	22.1	23.6	1.1
1000	unk			21.8	22.8	21.5	21.5	22.0	0.7
1200	19.9			20.0	21.8	20.5	19.0	20.1	1.1
(BI)	sfc 22.9	100 22.5	sfc 24.2	sfc 22.8	200 22.0	250 19.5	90 20.0	75 22.0	98 1.7
θ at BI	22.9	23.0	24.2	22.8	22.0	22.0	20.3	22.5	1.2
T_t	425 26.8	400 26.0	350 28.0	350 25.8	500 25.8	550 24.6	300 24.0	410 25.9	89 1.4
T_s	21.9	22.0	22.0	21.0	21.1	21.0	22.0	21.6	0.5
TI (°C)	+5.1	+4.0	+6.0	+4.8	+4.7	+3.6	+2.0	+4.3	1.3
Cloud Top(m)	350	UNK	350	UNK	245	230	UNK	238	08
Cloud Base(m)	haze	L. haze	L. haze	--	170	150		160	10
Surf Wind	270/07	270/07	--	--	--	**	--	270/07	0/0

*ave surf press 1014mb   ** wind aloft 090/25 at 1200 meters

Table A-II-b   Aircraft Data: Daily Digitized Analysis   4 Oct 76

Sounding	A	B	C	D	E	F	G	Mean	Std.Dev.
Lat N	32-31	32-13	32-07	32-27	33-07	33-36	33-02		
Lon W	117-09	117-02	117-03	117-13	118-01	118-20	117-47		
Time PDT	1412	1435	1500	1530	1611	1639	1704	1538	
Alt(m) T(°C)	▲	▲	▼	▲	▼	▲	▼		
(Bottom)	(3) 22.4	(3) 22.0	(3) 21.6	(60) 21.7	(3) 23.6	(3) 22.0	(3) 22.2	22.3	0.6
50	22.0	21.5	21.6	--	23.0	21.4	22.2	22.0	0.6
100	21.4	21.3	21.2	21.0	22.8	21.0	22.2	21.6	0.7
150	21.2	23.0	20.8	20.8	23.0	22.0	24.0	22.1	1.3
200	23.5	23.6	20.5	21.0	26.8	26.4	26.2	24.0	2.6
300	26.2	26.5	24.0	25.0	27.8	27.5	27.4	26.3	1.4
400	26.0	27.0	24.6	25.7	--	27.8	27.5	26.4	1.2
500	28.0	27.5	24.7	26.4	--	27.4	27.6	26.9	1.2
600	27.5	26.8	25.5	27.0	28.6	27.8	27.6	27.3	1.0
800		24.8	26.0	26.5	28.0	26.8	27.0	26.5	1.1
1000		24.0	25.0	24.6	27.0	25.2	25.8	25.3	1.0
1200		23.7	23.4	23.8	25.0	23.5	24.2	23.9	0.6
(BI)	165 21.2	105 21.3	205 20.5	180 20.7	160 23.0	130 20.5	140 22.5	155 21.4	33 1.0
θ at BI	22.9	22.3	22.5	22.5	24.6	21.8	23.9	22.9	1.0
T_t	500 28.0	480 27.6	800 26.0	600 27.0	600 28.6	380 28.0	700 27.7	580 27.6	140 0.8
T_s	22.0	19.7	21.7	21.2	22.2	20.9	21.9	21.4	0.9
TI (°C)	+6.0	+7.9	+4.3	+5.8	+6.4	+7.1	+5.8	+6.2	1.1
Cloud Top(m)	600	110	260	210	--	180	75	260	-
Cloud Base(m)	H. haze	H. hase	150	haze	--	haze	haze	150	-
Surf Wind	290/10	--	280/15	320/20	290/--	--	270/--	290/15	018/05

*ave surf press 1014 mb

Table A-II-c   Aircraft Data: Daily Digitized Analysis   5 Oct 76

Sounding	A	B	C	D	E	Mean	Std.Dev.
Lat N	32-47	32-52	32-44	33-03	33-01		
Lon W	117-17	117-29	117-32	118-35	118-31		
Time PDT	1504	1552	1612	1635	1710	1607	
Alt(m) T(°C) (Bottom)	(3) 19.0	(3) 20.0	(3) 21.0	(3) 21.0	(30) 21.0	20.5	1.0
50	18.5	19.5	20.0	21.0	21.0	20.0	1.1
100	18.0	18.5	19.0	21.0	21.0	19.5	1.4
150	18.0	17.5	19.0	21.0	20.0	19.1	1.4
200	18.0	17.0	18.5	21.0	20.0	18.9	1.6
300	23.0	19.0	19.0	22.0	20.0	20.6	1.8
400		22.0	26.0	27.0	26.0	25.3	2.2
500			27.0	27.5	27.0	27.2	0.3
600			26.5	27.8	27.0	27.1	0.7
800			26.0	27.5	28.5	27.3	1.3
1000			25.0	26.5	27.0	26.8	1.2
1200			24.0	26.0	26.0	25.3	1.2
(BI)	200	200	250	230	300	235	42
θ at BI	18.0 20.0	17.0 19.0	18.0 20.5	21.0 23.3	20.0 23.0	18.8 21.2	1.6 1.9
T_t	N/A	N/A	500 27.0	700 28.0	880 29.0	695 28.0	190 1.0
T_s	22.5	22.2	22.1	21.3	21.8	22.0	0.5
$\overline{TI}$ (°C)	--	--	+4.9	+6.7	+6.2	+5.9	0.9
Cloud Top(m)	200	350	270	275	270	278	53
Cloud Base(m)	100	80	75	75	90	84	11
Surf Wind	230/10	--	--	250/--	--	270/10	

ave surf press*1013 mb

Table A-II-d   Aircraft Data: Daily Digitized Analysis   6 Oct 76

71

Table A-II-e   Aircraft Data: Daily Digitized Analysis   7 Oct 76

Sounding	A	B	C	D	E	F	G	H	I	J	Mean	Std.Dev.
Lat N	32-54	34-00	34-13	34-17	34-34	34-31	34-23	34-22	33-41	32-59		
Lon W	117-22	119-31	119-48	120-13	120-50	120-41	120-30	120-06	118-35	117-48		
Time PDT	1415	1535	1550	1609	1630	1640	1651	1715	1755	1819	1630	
Alt(m) T(°C)												
50 (Bottom)	(365)29.0	(3)18.0	(3)17.0	(3)18.0	(3)19.8	(3)19.0	(60)19.0	(105)23.0	(3)21.0	(3)20.0	19.6	2.1
100	--	17.5	17.0	17.8	18.5	18.0	--	--	20.0	20.0	18.4	1.2
150	--	17.0	17.0	18.0	18.0	18.0	18.5	--	19.0	20.0	18.2	1.0
200	--	19.5	20.2	20.0	19.5	18.0	19.6	24.5	19.5	21.5	20.1	2.0
250	--	22.0	22.0	22.0	22.5	19.5	26.0	26.0	23.5	25.0	22.5	2.5
300	--	25.0	25.0	27.0	26.4	22.0	26.8	27.8	30.0	28.0	27.1	2.6
400	29.0	28.5	27.5	28.0	27.8	25.0	27.8	28.0	30.8	30.0	28.2	1.7
500	29.6	30.0	28.5	28.0	28.5	27.6	28.5	28.5	30.5	30.0	28.8	1.1
600	28.5	29.0	28.5	28.0	27.0	27.0	29.0	27.8	29.0	30.0	28.4	0.9
800	27.0	28.5	26.8	27.5	27.0	27.0	28.8	26.6	26.8	28.2	27.4	0.8
1000	25.5	26.0	25.0	25.5	26.0	25.7	26.0	25.4	25.4	26.0	25.7	0.3
1200	24.0	23.0	23.0	23.0	25.0	24.0	24.0	24.0	24.0	24.0	23.7	0.8
(BI)	--	100	100	115	160	160	120	--	180	130	135	30
θ at BI	--	17.0	18.0	18.0	19.6	19.6	19.2	--	21.3	21.3	19.5	1.3
T_t	400 29.0	500 30.0	550 29.0	500 28.0	480 28.0	450 27.0	530 29.0	430 29.0	420 31.0	400 30.0	470 29.0	55 1.2
T_s	21.4	20.4	20.4	19.2	19.0	18.0	18.0	20.5	21.8	21.6	20.0	1.4
ΔT	+.76	+9.6	+8.6	+8.8	+9.0	+9.0	+11.0	+8.5	+9.2	+8.4	+9.0	0.9
Cloud Top(m)	--	--	--	--	--	240	200	--	180	130	220	20
Cloud Base(m)	--	--	--	55	55	90	fog	--	haze	haze	48	45
Surf Wind	--	--	--	330/20	310/20	--	--	--	--	290/--	310/20	020/00

*ave surf press 1012 mb

Sounding lat N Lon W Time PDT Alt(m) T(°C)	A 33-13 117-25 1300	B 33-23 117-40 1309	C 33-24 118-12 1322	D 33-35 118-38 1329	E 34-16 119-33 1404	F 34-22 120-33 1603	G 34-38 120-42 1618	H 34-45 121-08 1632	I 35-01 121-26 1717	J 34-57 121-19 1728	K 34-43 120-44 1809	Mean 1530	Std.D
(Bottom)	(3) 24.0	(3) 26.0	(3) 27.0	(60) 30.5	(3) 25.5	(3) 23.0	(3) 22.0	(3) 22.0	(3) 18.5	(3) 19.0	(15) 20.0	23.5	3.7
50	29.5	28.0	29.0	--	27.0	25.0	24.5	21.5	17.8	18.5	20.0	24.1	4.4
100	31.0	29.5	29.5	30.0	28.2	28.3	25.0	22.0	19.0	18.1	20.0	25.5	4.9
150	32.0	29.8	29.8	30.0	28.5	28.8	23.0	25.5	23.0	26.0	23.0	26.9	3.7
200	32.5	30.0	30.0	29.5	29.0	29.2	24.0	26.2	27.0	28.8	26.0	27.9	2.8
300	31.2	29.8	29.5	29.0	30.0	29.5	28.0	27.0	27.5	27.5	26.3	28.6	1.6
400	30.0	29.5	29.0	30.0	29.5	29.5	28.0	27.7	28.2	28.2	27.2	28.7	1.1
500	29.0	29.1	28.5	29.0	29.0	29.0	28.0	28.0	29.0	28.6	27.2	28.6	0.6
600	28.0	28.8	28.0	28.2	28.5	28.7	28.0	28.0	28.6	28.0	26.0	28.1	0.4
800	26.4	27.7	26.7	26.7	27.3	27.5	28.2	27.0	26.6	26.6	26.0	27.0	0.6
1000					25.8	26.8	27.0	26.6	26.0	25.2	25.6	26.1	0.7
1200					23.8	26.0	26.0	25.5	22.2	24.0	24.0	24.9	1.0
(BI)	sfc 24.0	sfc 26.0	sfc 27.0	-- --	sfc 25.5	sfc 23.0	sfc 22.0	70 21.0	85 17.2	120 18.0	160 20.0	45 22.4	60 3.3
θ at BI	24.0	26.0	27.0	--	25.5	23.0	22.0	21.7	18.1	19.2	21.6	22.8	2.9
Tt	200 32.5	200 30.0	200 30.0	60 30.5	300 30.0	350 29.5	750 28.5	550 28.0	500 29.0	450 29.0	550 27.5	505 29.5	205 1.4
Ts	22.2	22.8	22.2	23.8	21.8	19.4	19.2	18.0	18.3	18.3	16.4	20.2	2.4
TI	+10.3	+7.2	+7.8	+6.2	+8.2	+10.1	+9.3	+10.0	+10.2	+10.7	+11.1	+9.3	1.5
Cloud Top(m)	200	30	80	--	--	--	40	1500	1500	1500	1500	40	--
Cloud Base(m)	haze	H. haze	L. haze	--	--	--	fog	L. haze	L. haze	L. haze	L. haze	fog	--
Surf Wind	calm	--	--	calm	330/2	300/--	285/--	--	310/--	--	--	305/09	--

*ave surf press 1014 mb   ** wind aloft   090/20 at 2000 meters at 1901 PDT

Table A-II-f   Aircraft Data: Daily Digitized Analysis   8 Oct 76

Sounding	A	B	C	D	E	F	G	Mean	Std.Dev.
Lat N	33-26	33-22	33-15	33-01	32-50	32-47	32-45		
Lon W	117-46	118-03	118-20	118-20	118-19	118-12	117-21		
Time PDT	▲ 1107	▼ 1120	▲ 1132	▼ 1150	▲ 1214	▼ 1222	▲ 1240	1155	
Alt(m) T(°C) (Bottom)	(30)24.0	(3)25.0	(3)26.0	(3)25.0	(6)25.0	(6)26.0	(90)29.0	25.2	0.7
50	29.0	27.0	27.0	29.0	29.5	31.0	--	28.8	1.5
100	28.0	31.0	27.0	29.5	30.2	31.0	29.5	29.5	1.5
150	30.2	30.0	30.0	30.0	29.8	30.7	30.3	30.1	0.3
200	30.6	30.0	31.0	31.0	29.5	30.5	31.0	30.5	0.6
300	30.5	30.0	30.5	30.5	29.0	30.0	30.2	30.1	0.5
400	29.8	29.3	30.0	30.1	28.3	29.4	29.6	29.5	0.6
500	29.0	28.7	29.6	29.8	27.8	28.4	28.7	28.9	0.7
600	28.2	28.0	29.2	29.2	27.0	27.0	28.0	28.1	0.9
800			27.5	28.0			26.5	27.4	0.8
1000			26.1	27.4				26.8	0.9
1200			24.5	25.0				24.8	0.4
(BI)	sfc 24.0	sfc 25.0	sfc 26.0	sfc 25.0	sfc 25.1	sfc 26.1	-- --	sfc 25.2	00 0.8
θ at BI	24.0	25.0	26.0	25.0	25.1	26.1	-- --	25.2	0.8
Tt	250 30.8	100 31.0	200 31.0	200 31.0	80 30.6	75 31.0	200 31.0	160 30.9	70 0.2
Ts	21.3	21.8	22.0	21.9	22.0	22.0	21.8	21.8	0.2
TI	+9.5	+9.2	+9.0	+9.1	+8.6	+9.0	+9.2	+9.1	0.3
Cloud Top(m)	none	--	none	none	none	none	none	clear	
Cloud Base(m)	--	L. haze	--	--	--	--	--	clear	
Surf Wind	calm	calm	--	--	--	calm	--	calm	

*ave surf press 1011 mb

Table A-II-g   Aircraft Data: Daily Digitized Analysis   9 Oct 76

Sounding	A	B	C	D	E	F	G	H	I	J
Lat N	32-43	32-38	32-38	32-35	32-33	32-38	33-02	33-15	33-17	33-22
Lon W	117-17	117-18	117-24	117-25	117-33	117-26	117-27	117-31	117-45	117-43
Time PDT	1309	1316	1325	1332	1340	1348	1406	1412	1422	1427
Alt(m) T(°C)										
(Bottom)	(3) 22.5	(3) 22.5	(3) 23.0	(3) 22.5	(3) 22.0	(3) 21.0	(3) 21.0	(3) 21.0	(3) 21.0	(3) 20.0
50	21.0	22.5	22.2	22.0	21.0	21.0	21.0	20.2	21.0	20.0
100	21.0	21.0	22.0	22.0	21.0	21.2	23.0	20.0	22.8	21.5
150	23.0	22.8	23.5	24.8	23.5	24.2	25.0	24.7	24.6	24.6
200	24.3	25.0	27.0	26.4	26.2	25.4	25.7	26.5	27.0	27.4
300	27.0	26.7	27.0	27.5	27.0	27.0	27.4	27.0	27.7	27.7
400		27.0	26.5	28.5	28.0	27.8	27.7	28.0	28.0	28.0
500		27.0	27.5	27.7	28.1	27.4	27.9	28.0	28.0	28.0
600		26.0	25.8	27.0	27.5	27.1	27.7	28.0	28.0	28.0
800		25.0	26.1	26.0	25.7	26.4	26.4	26.3	26.6	26.4
1000							24.8			24.8
1200										23.0
(BI)	100 21.0	100 22.0	130 22.0	130 22.0	130 21.0	90 21.0	85 21.0	105 20.0	75 21.0	75 20.0
θ at BI	22.0	22.0	23.3	23.3	22.3	21.9	21.9	21.1	21.8	20.8
T^t	300 27.0	450 27.5	400 27.5	370 28.8	500 28.1	370 28.0	550 28.0	640 28.1	550 28.0	500 28.0
T_s	22.3	22.4	22.7	22.7	22.7	22.7	22.2	22.3	21.5	21.5
TI	+4.7	+5.1	+4.8	+6.1	+5.4	+5.3	+5.8	+5.8	+6.5	+6.5
Cloud Top(m)	--	145	137	70	140	110	105	105	105	105
Cloud Base(m)	--	haze	haze	H. fog	haze	fog	15	H. fog	haze	H. fog
Surf Wind	calm	230/2	--	--	250/--	--	--	--	220/--	270/--

*ave surf press 1012 mb

Table A-II-h   Aircraft Data: Daily Digitized Analysis   10 Oct 76 (part 1)

Sounding	K	L	M	N	O	P	Q	R	Mean	Std.Dev.
Lat N	34-03	33-58	34-23	34-16	34-09	34-18	32-52	32-50		
Lon W	119-14	119-04	120-28	120-39	120-28	120-35	117-23	117-17		
Time PDT	1516	1526	1605	1619	1624	1639	1800	1809	1540	
Alt(m) T(°C)										
(Bottom)	(6) 20.0	(10)19.0	(3) 17.5	(10)17.0	(15)16.5	(10)16.0	(3) 22.0	(3) 22.0	20.4	2.3
50	20.0	18.8	17.4	16.7	16.8	16.0	21.3	21.6	20.0	2.0
100	20.0	18.3	18.0	16.5	17.0	16.0	20.7	20.8	20.2	2.1
150	21.8	23.2	19.8	16.5	16.8	19.5	20.0	20.2	22.1	2.7
200	24.3	24.5	23.0	17.0	19.5	22.5	22.7	22.0	24.2	2.8
300	26.2	26.4	25.8	24.0	23.2	24.8	25.0	25.0	26.3	1.3
400	27.8	28.0	25.8	25.0	26.0	26.2	26.2	26.0	27.1	1.1
500	27.9	28.0	25.9	27.0	26.8	26.5	26.4	26.0	27.3	0.8
600	27.5	27.4	26.0			26.5	26.0		27.1	0.7
800	25.8	25.9	25.8			26.5			26.1	0.3
1000	24.7	24.5	25.1			24.8			24.8	0.2
1200	22.8	23.0	22.6			23.2			22.9	0.2
(BI)	120 20.0	100 18.3	90 17.3	170 16.5	140 16.5	140 16.0	150 20.0	150 20.2	115 19.7	28 1.9
θ at BI	21.2	19.3	18.2	18.2	17.9	17.4	21.5	21.7	20.9	1.9
Tt	480 28.0	450 28.0	330 26.3	500 27.0	500 26.8	600 26.5	450 26.8	460 26.5	465 27.5	90 0.7
Ts	22.3	22.4	18.4	18.2	18.0	18.0	23.0	22.4	21.4	1.8
TI	+5.7	+5.6	+7.9	+8.8	+8.8	+8.5	+3.8	+4.1	+6.1	1.5
Cloud Top(m)	140	135	120	180	180	160	200	150	130	42
Cloud Base(m)	haze	H. fog	H. haze	90	90	90	105	haze	40	47
Surf Wind	--	--	315/15	--	--	--	--	--	260/09	038/09

*ave surf press 1012 mb

Table A-II-h   Aircraft Data: Daily Digitized Analysis   10 Oct 76
(part 2)

76

Sounding	A	B	C	D	E&F	G	H	I	J	K	Mean	Std.Dev.
Lat N	32-58	32-41	32-07	32-28	32-53	32-38	32-56	32-51	32-55	32-53		
Lon W	117-48	117-48	117-48	118-15	117-56	117-34	117-24	117-18	117-20	117-23		
Time PDT	1443	1444	1527	1444	1642	1703	1741	1745	1750	1759	1620	
Alt(m) T(°C) (Bottom)	(3) 20.0	(3) 20.5	(15) 19.0	(6) 20.0	(30) 21.0	(45) 20.5	(3) 22.0	(3) 21.0	(3) 21.0	(3) 21.0	20.7	0.8
50	19.5	20.0	18.8	19.0	20.5	20.3	21.6	20.6	20.6	21.0	20.2	0.9
100	19.2	19.6	18.5	19.0	20.0	20.0	21.0	20.1	20.1	21.0	19.9	0.8
150	19.0	19.0	18.2	18.6	19.5	19.5	20.4	19.0	19.6	20.2	19.3	0.7
200	19.0	18.5	17.5	18.1	19.0	19.0	20.0	19.0	19.0	19.7	18.9	0.7
300	23.5	23.2	17.0	17.0	21.0	22.6	20.0	20.0	19.8	20.0	20.4	2.2
400	23.8	24.2	21.0	17.0	25.0	24.4	24.5	23.5	23.0	23.2	23.0	2.4
500	24.0	24.5	23.0	24.0	24.6	24.2	24.8	24.0	23.0	24.0	24.0	0.6
600	24.0	25.0	24.0	24.0	24.3	25.0	24.5		23.2	23.0	24.1	0.7
800	23.5	24.0	23.2	23.0	23.4	23.5	23.6				23.5	0.3
1000	22.0	22.5	22.6	22.0	22.3	22.3	22.6				22.3	0.3
1200		21.0	21.0	21.5	21.2	21.2	21.6				21.3	0.3
(BI)	240 19.0	240 18.3	340 17.0	400 17.0	240 18.8	240 18.8	300 20.0	240 19.0	275 18.5	220 19.2	275 18.5	57 1.0
θ at BI	21.4	20.7	20.4	21.0	21.2	21.2	23.0	21.4	20.8	21.4	21.3	0.7
Γ_L	550 24.0	600 25.0	600 24.0	550 24.0	400 25.0	600 25.0	480 25.0	500 24.0	600 23.2	500 24.0	440 24.3	68 0.6
Γ_u	22.8	22.8	21.0	21.3	22.0	21.4	22.5	22.1	22.1	22.2	22.0	0.6
Ti	+1.2	+2.2	+3.0	+2.7	+3.0	+3.6	+2.5	+1.8	+1.1	+1.8	+2.3	0.8
Cloud Top(m)	150	150	400	440	300	--	210	260	260	230	440	--
Cloud Base(m)	haze	haze	haze	270	haze	--	haze	haze	haze	haze	270	--
Surf Wind	--	--	260/--	--	--	--	--	--	--	--	260/--	

*ave surf press 1014 mb

Table A-II-i   Aircraft Data: Daily Digitized Analysis   11 Oct 76

Sounding	A	B	C	Mean	Std.Dev.
Lat N	32-39	32-55	32-46		
Lon W	117-15	117-22	117-26		
Time PDT	1516	1530	1552	1535	
Alt(m) $T(°C)$					
(Bottom)	(3) 22.0	(30) 22.0	(3) 22.0	22.1	0.2
50	21.7	21.8	21.8	21.8	0.1
100	21.3	21.0	21.4	21.2	0.2
150	20.9	20.5	20.8	20.7	0.2
200	20.4	20.0	20.2	20.2	0.2
300	19.5	19.0	19.0	19.2	0.3
400	21.8	18.5	18.5	19.6	1.9
500	21.4	25.2	27.7	24.8	3.2
600		27.8	27.3	27.6	0.4
800		26.3		26.3	--
1000		25.8		25.8	--
1200		23.8		23.8	--
(BI)	300 19.5	400 18.5	400 18.5	365 18.8	58 0.6
θ at BI	22.5	22.5	22.5	22.5	0
T_t	-- --	580 28.0	500 27.7	540 27.9	40 0.2
T_s	20.7	21.8	22.0	21.5	0.7
T_I	--	+6.2	+5.7	+5.0	0.4
Cloud Top(m)	365	420	420	420	0
Cloud Base(m)	haze 200	200	--	200	0
Surf Wind	280/10	--/--	--/--	280/10	

*ave surf press 1014 mb

Table A-II-j   Aircraft Data: Daily Digitized Analysis   12 Oct 76
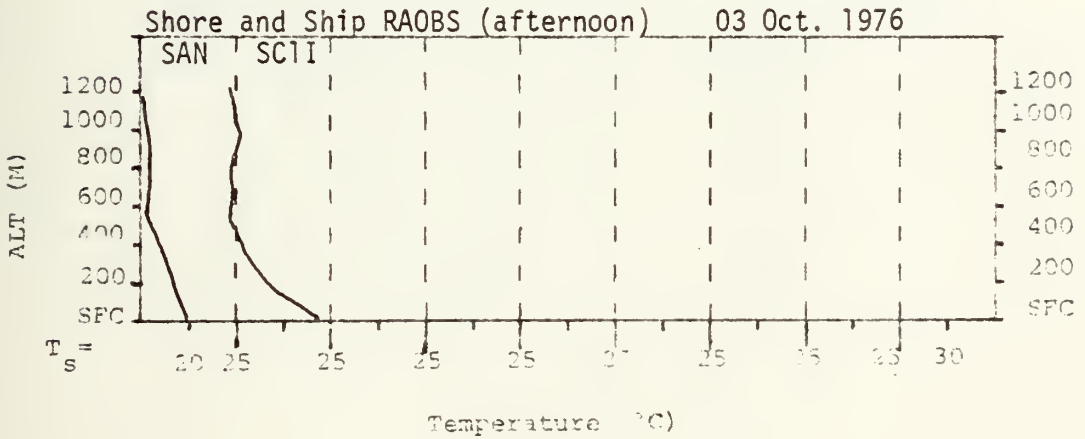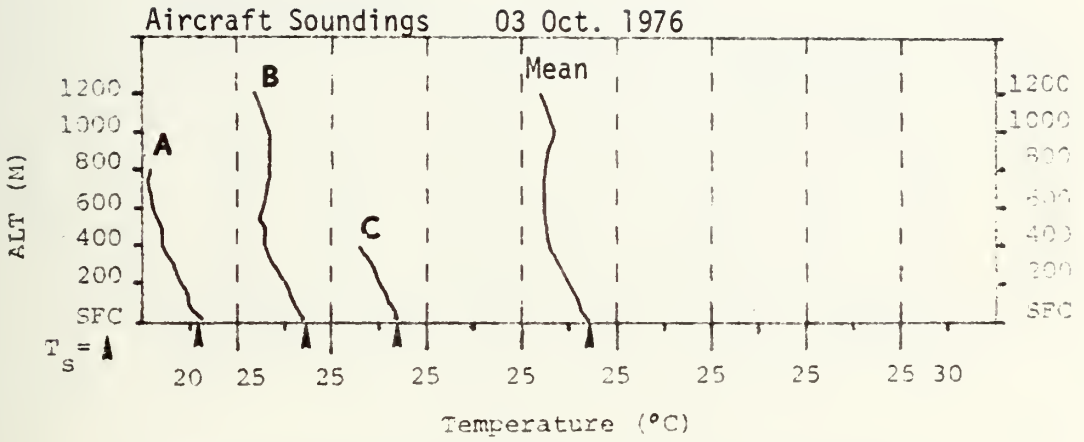
Figure A-3-a   Aircraft Soundings   3 Oct
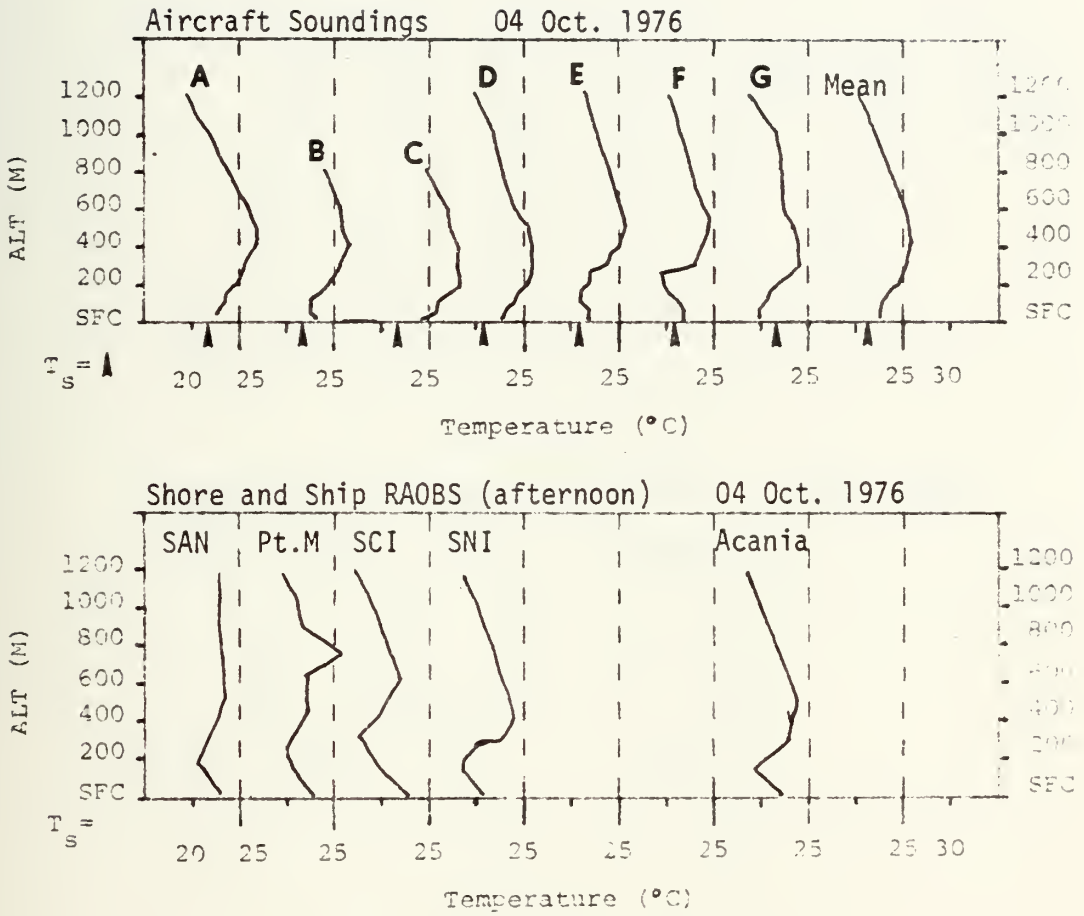
Figure A-3-b   Aircraft Soundings   4 Oct.
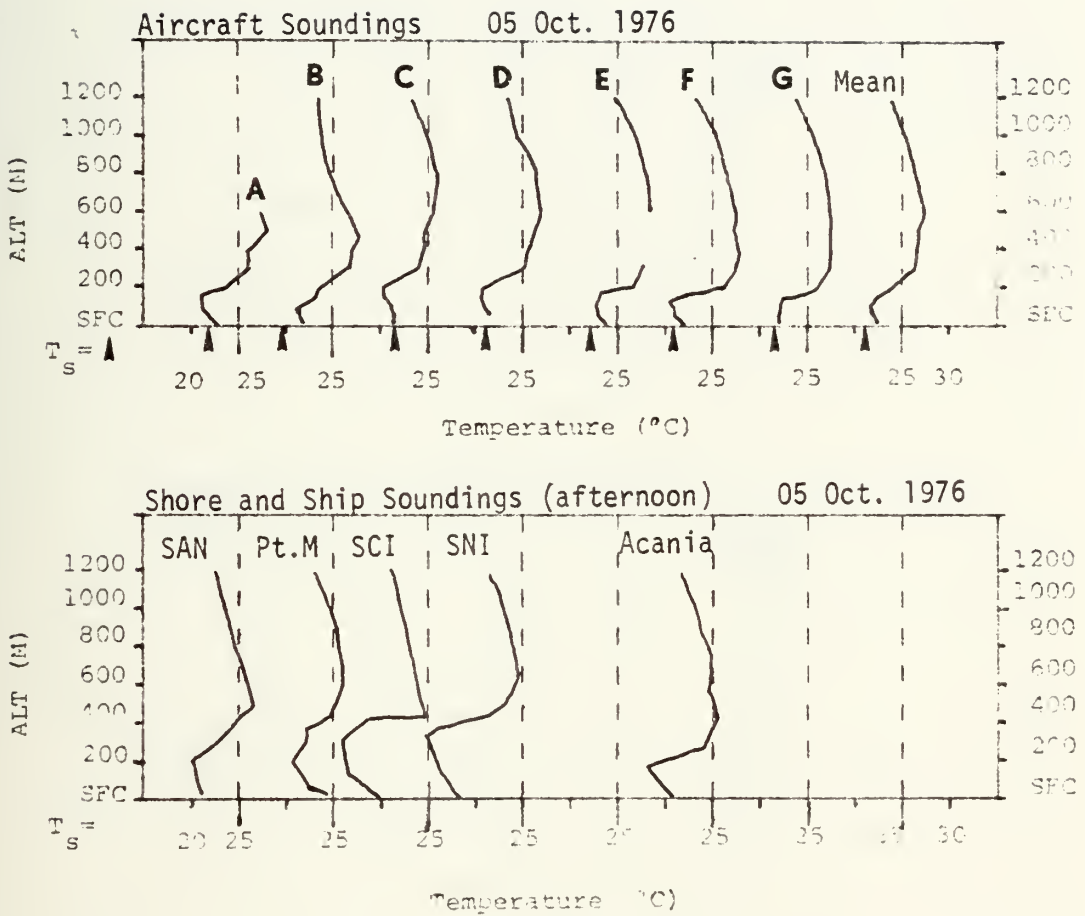
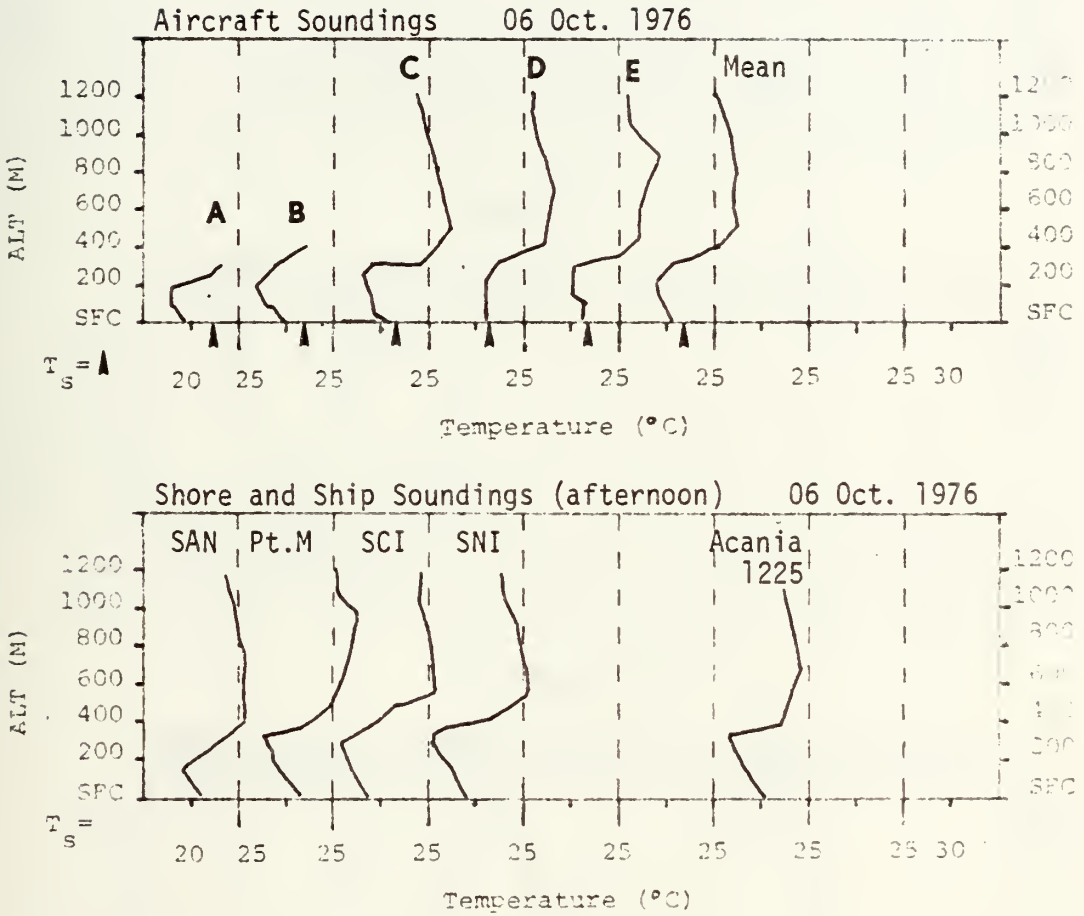Figure A-3-c   Aircraft Soundings   5 Oct
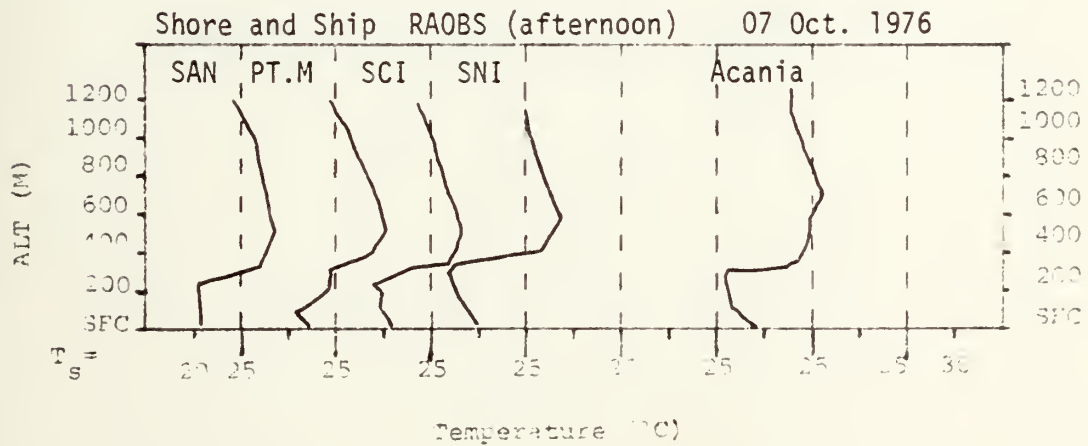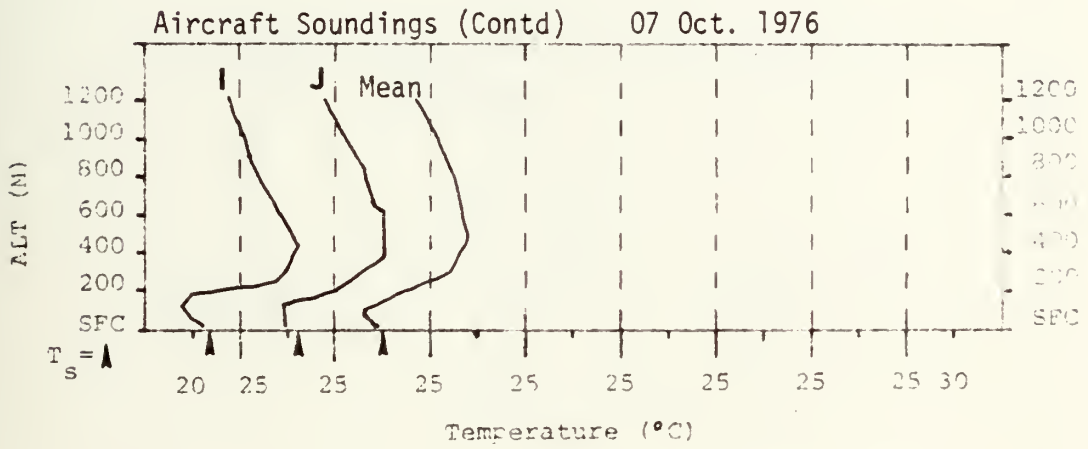
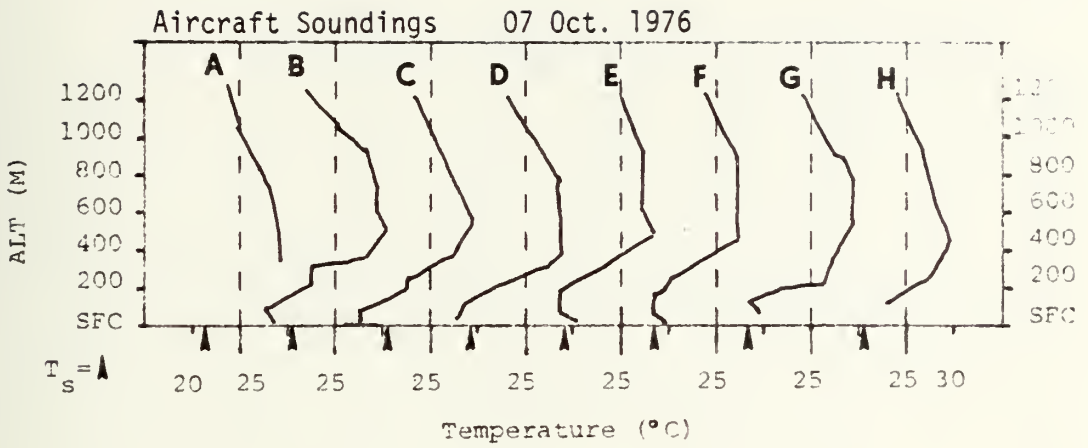Figure A-3-d   Aircraft Soundings   6 Oct

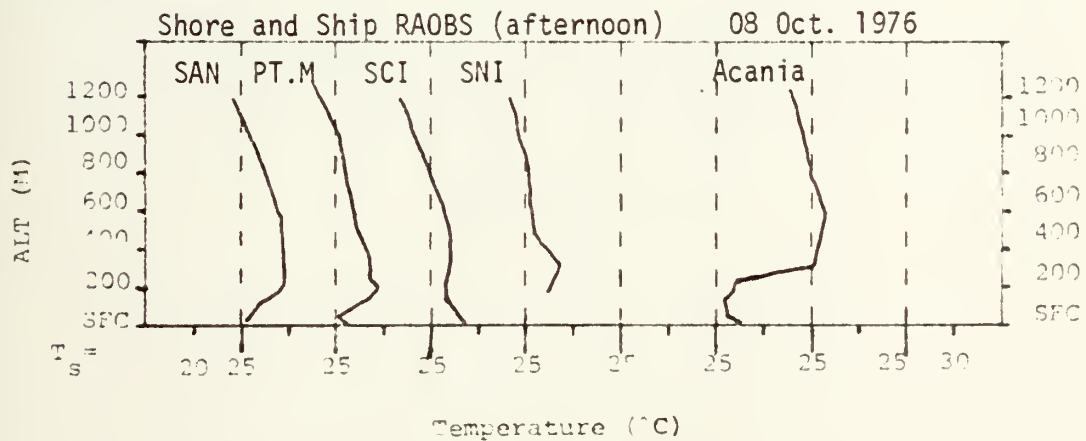Figure A-3-e   Aircraft Soundings   7 Oct
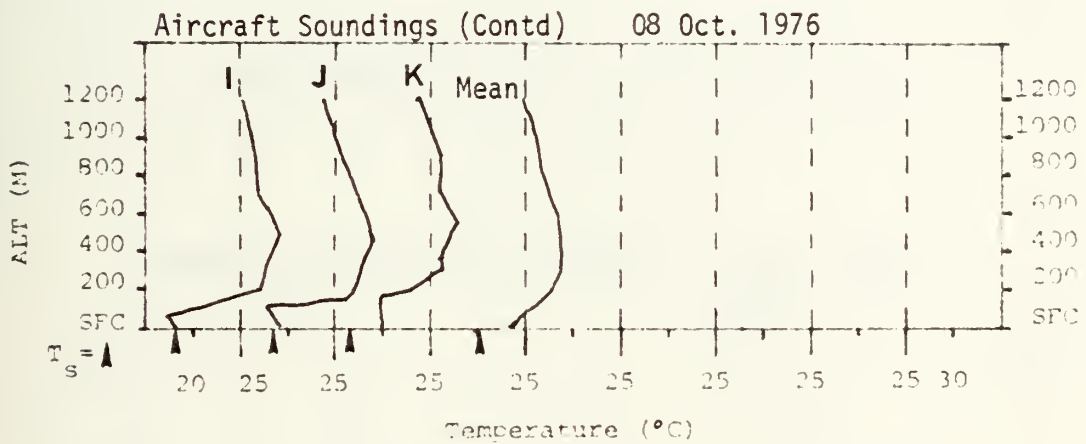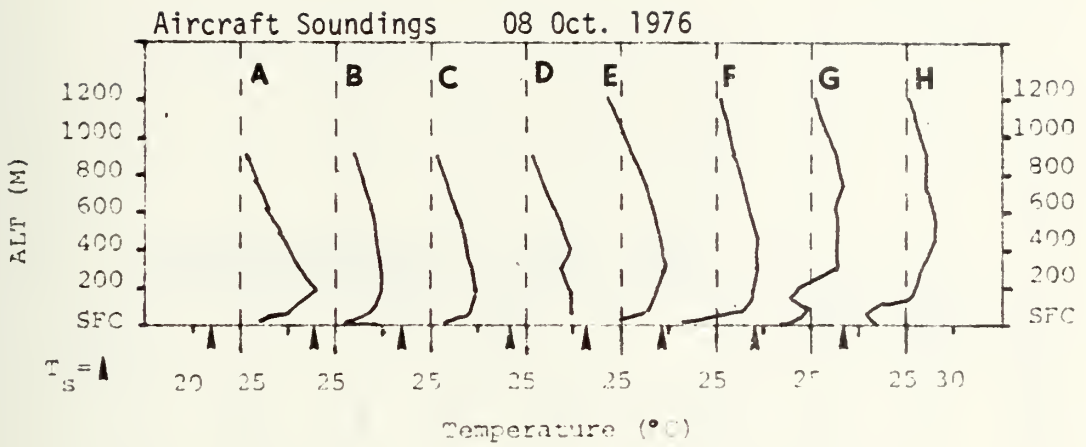
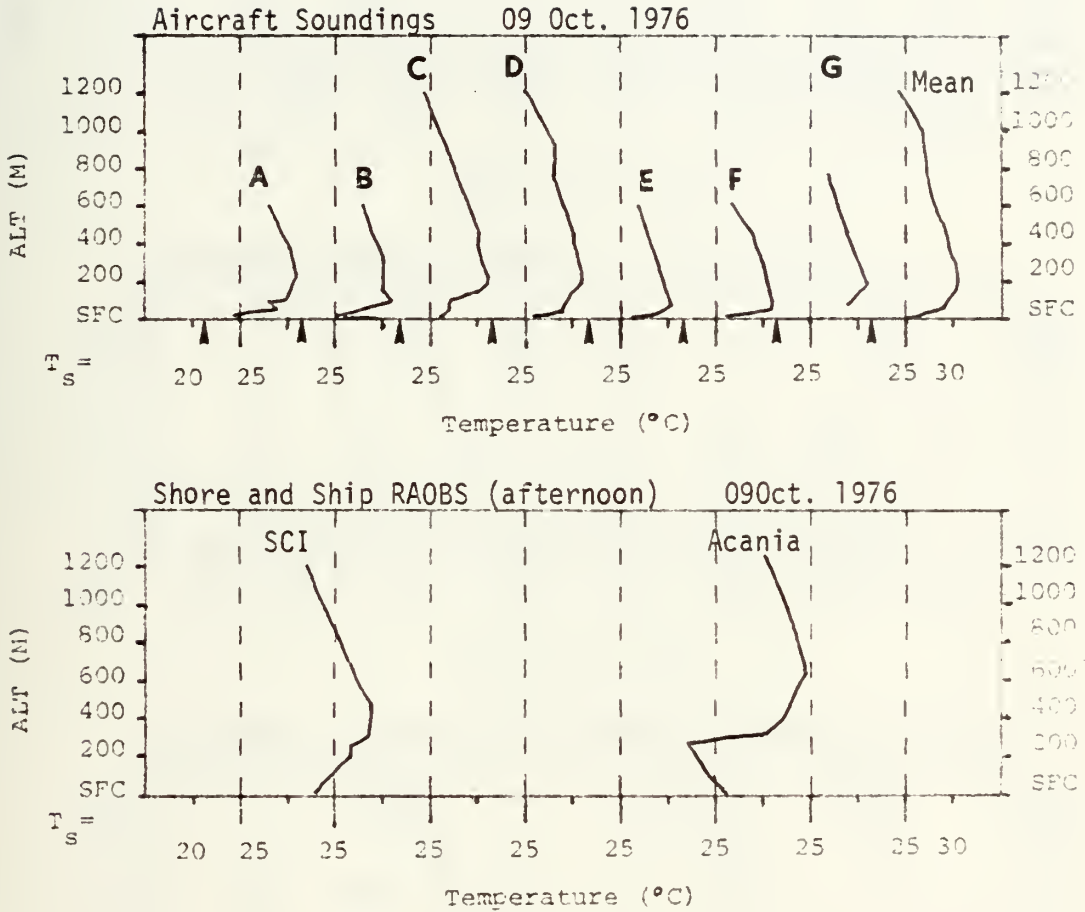Figure A-3-f   Aircraft Soundings   8 Oct

Figure A-3-g   Aircraft Soundings   9 Oct

Figure A-3-h   Aircraft Soundings   10 Oct

Figure A-3-i   Aircraft Soundings   11 Oct

Figure A-3-j   Aircraft Soundings   12 Oct

NPS-NELC

CEWCOM 76

Aircraft Soundings
Sounding / B.I.(m)
T.I.(°C) / T_w (°C)
▲ (Position)

Shore Station
FOG ?
B.I.(m)
T.I.(°C)
M.I.(°C)
RH(p/μ)

No Fog
- - -

No Fog
- -
- -4.5

No Fog
755
-5.0
-5.5
1.04

No Fog
- -
- -3.7
- -

A1638 none
0.0 21.3
B1821 none
-0.1 23.5
C1842 unk
+0.2 22.

1800 PDT

Cu
or St

Haze

Wisps

Wisps

Wisps

Clear

Clear

Pt. Arguello
Pt. Conception

Pt. Mugu

Los Angeles

San
Diego

S.N.I.

S.R.I.

S.C.I.

A.I.

S.B.I.

Markson Obs. →

1015 SMS-2 →

⊕ St

⊕ St

⊕ St

⊕ St

N

3 Oct

Indices and Weather Depiction

Figure A-4-a

NPS-NELC

CEWCOM 76

Aircraft Soundings

Sounding / B.l.(m)
T.1.(°C) / T_w (°C)
▲ (position)

Shore Station

FOG ?

H.1.(m)
T.1.(°C)
M.1.(°C)
M1(g/kg)

Fog
3/258
+.6
-1.8
0.38

C1710 sfc
16.0 22.0

G1850 90
+2.0 22.0

A1628 sfc
+5.1 21.9

B1648 100
+4.0 22.0

D172▲ sfc
+4.8 21.0

al 1200 m

Row Stratus
F1822 250
+3.6 21.0

S.B.I. ▲250
21.1

E1806 ▲250
+4.2

No Fog
34/309
+1.5
-2.4
1.64

San Diego

L.C.I.

Acania
0347
305
-2.9
-2.6
1.92

L. Haze

⊕ st

No Fog
264
+1.2
-4.3
1.1

⊕ st

⊕ St

No Fog
174
+3.4
-3.2
1.04

⊕St

⊕ st

Clear

Pt. Arguello
Pt. Conception

Pt. Mugu

Los Angeles

S.M.I.

A.I.

S.R.I.

Markson Obs   ⌒→
1030 DMSP   — — —

-N-

Indices and Weather Depiction

Figure A-4-b

90

Figure A-4-c   Indices and Weather Depiction

NPS-NELC

CEWCOM 76

Figure A-4-d   Indices and Weather Depiction   6 Oct

NPS-NELC

CEWCOM 76

Aircraft Soundings
Sounding / B.I.(m)
T.I.(°C) / T_w(°C)
▲ (Position)

Shore Station
FOG ?
B.I.(m)
T.I.(°C)
M.I.(°C)
M3(g/kg)

419
+7.2
-1.7
2.09
No Fog

San Diego

L.C.I.

A4415 unk 21.4
+7.6

1800Kow
PDT Stratus

1400 PST

⊕ St

J1819 030
+8.4 ↑7.6

Los Angeles

Haze

No Fog
244
+7.2
-5.1
2.61

⊕ St

Fog
324
+17.6
-1.1
1.15

Pt. Mugu

I1755 ▲180 21.8
+9.2

S.B.I.

⊕ St

⊕ St

S.N.I.

⊕ St

Fog
423
+7.3
-2.7
0.11

Pt. Conception

Pt. Arguello

I1715 unk 20.5
+8.5 ▲

B1535 ↑00 20.4
+9.6

C1550 ▲00 20.4
+8.6

D1609 115 19.2
+8.8 ▲

S.R.I.

S.M.I.

FOG

FOG

⊕ St

Fog
423
+6.3
-2.5
2.03

AcanTe
0400
+6.3
-2.5
2.03

Markson Obs. (1800) →

Markson Obs. →

1110 DMSP →

E1630 16.0
+9.0 19.0 F1640 ▲66 18.0
+9.0

⊕ St

G1651 120 18.0
+11.0

— N —

Figure A-4-e   Indices and Weather Depiction

7 Oct

93

Figure A-4-f   Indices and Weather Depiction

NPS-NELC

CEWCOM 76

Shore Station
FOG ?
B.I. (m)
T.I. (°C)
M.I. (°C)
MR(p/kg)

Aircraft Soundings
Sounding / B.I. (m)
T.I.(°C) / T_w (°C)
▲ (Position)

● Los Angeles

Pt. Arguello
Pt. Conception

S.M.I.
S.R.I.
A.I.
S.Cr.I.

Pt. Mugu

No Fog
—
—
-6.7
—

Clear

S.B.I.

No Fog
—
—
-7.6
—

Acania
0350
87
+8.5
-3.4
2.17

⊕ High Cloud

Markson Obs. → 1005 DMSP

⊕ St

-N-

Clear

No Fog
—4
+8.0
-8.2
2.49

Clear

A1107 sfc
+9.5 21.3

B1120 sfc
+9.2 21.8

Wind calm

C1132 ▲ sfc
+9.0   22.0

D1150 ▲ sfc
9.1   21.9

F1222 sfc
+9.0 22.0

E1214 sfc
+8.6   22.0

S.N.I.

S.C.I.

No Fog
— — — —

San Diego

G1240 unk
+9.2 21.8

L.C.I.

20 - 30 m
Very Shallow Haze

Indices and Weather Depiction   9 Oct

Figure A-4-g

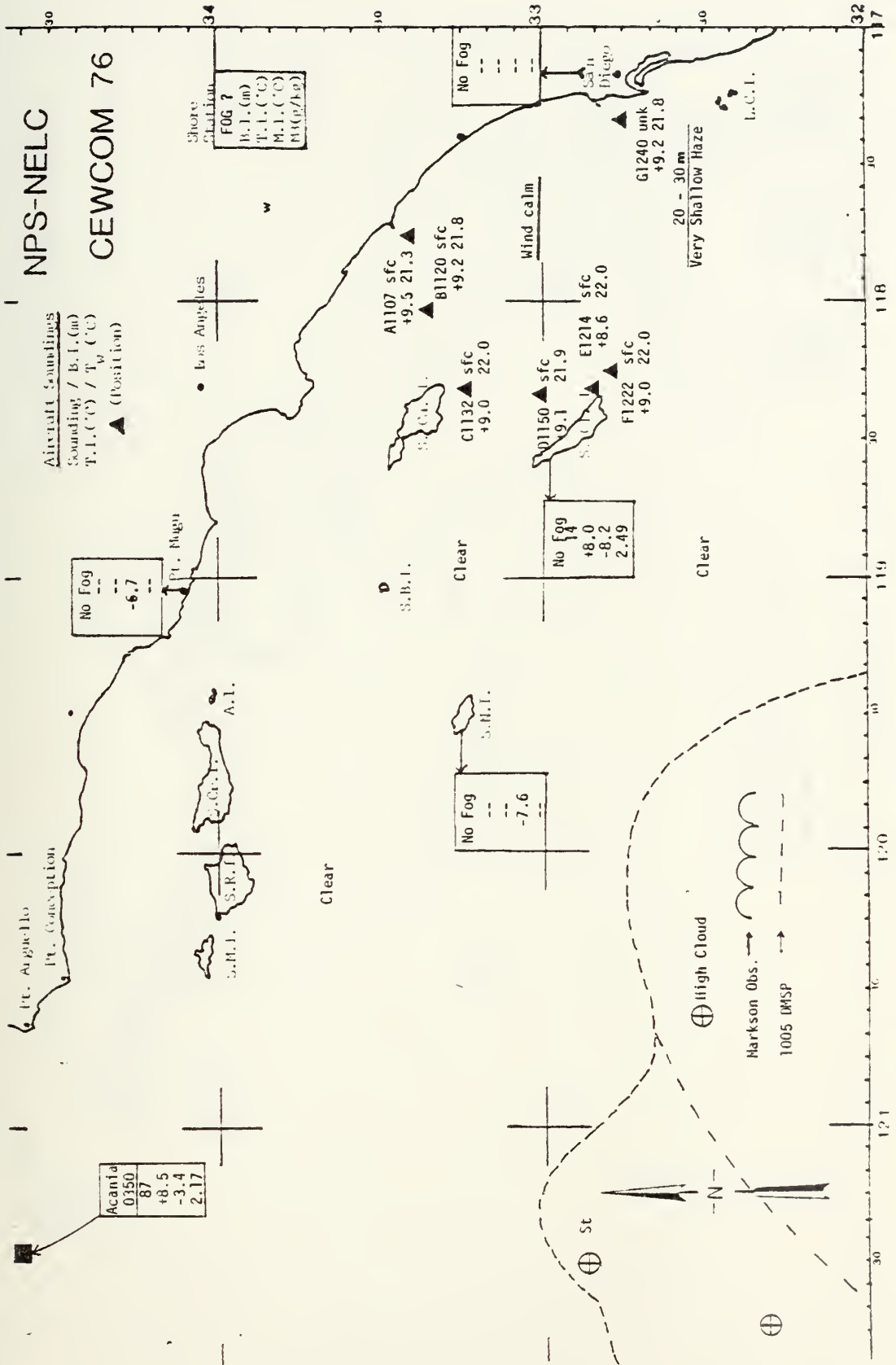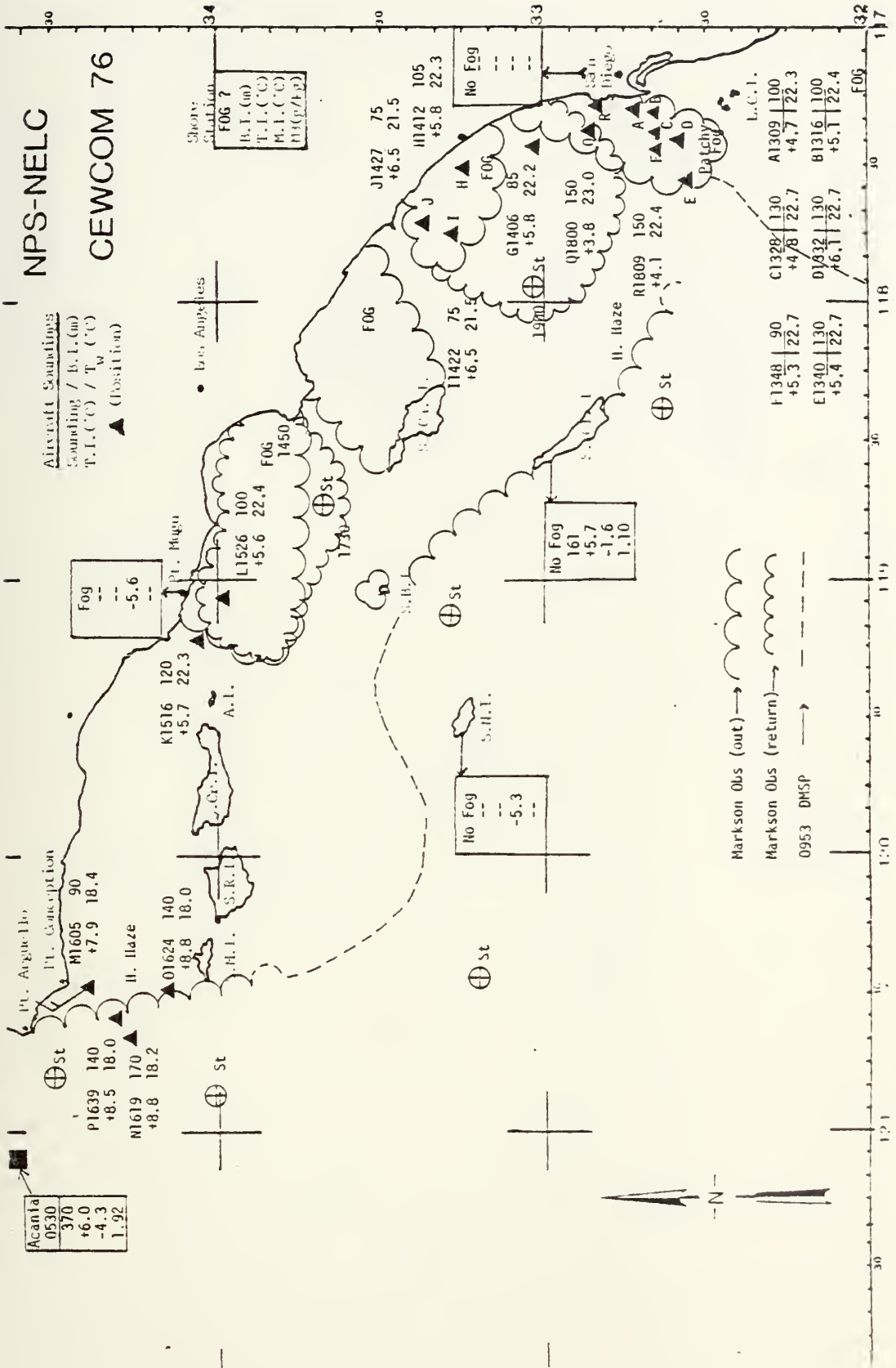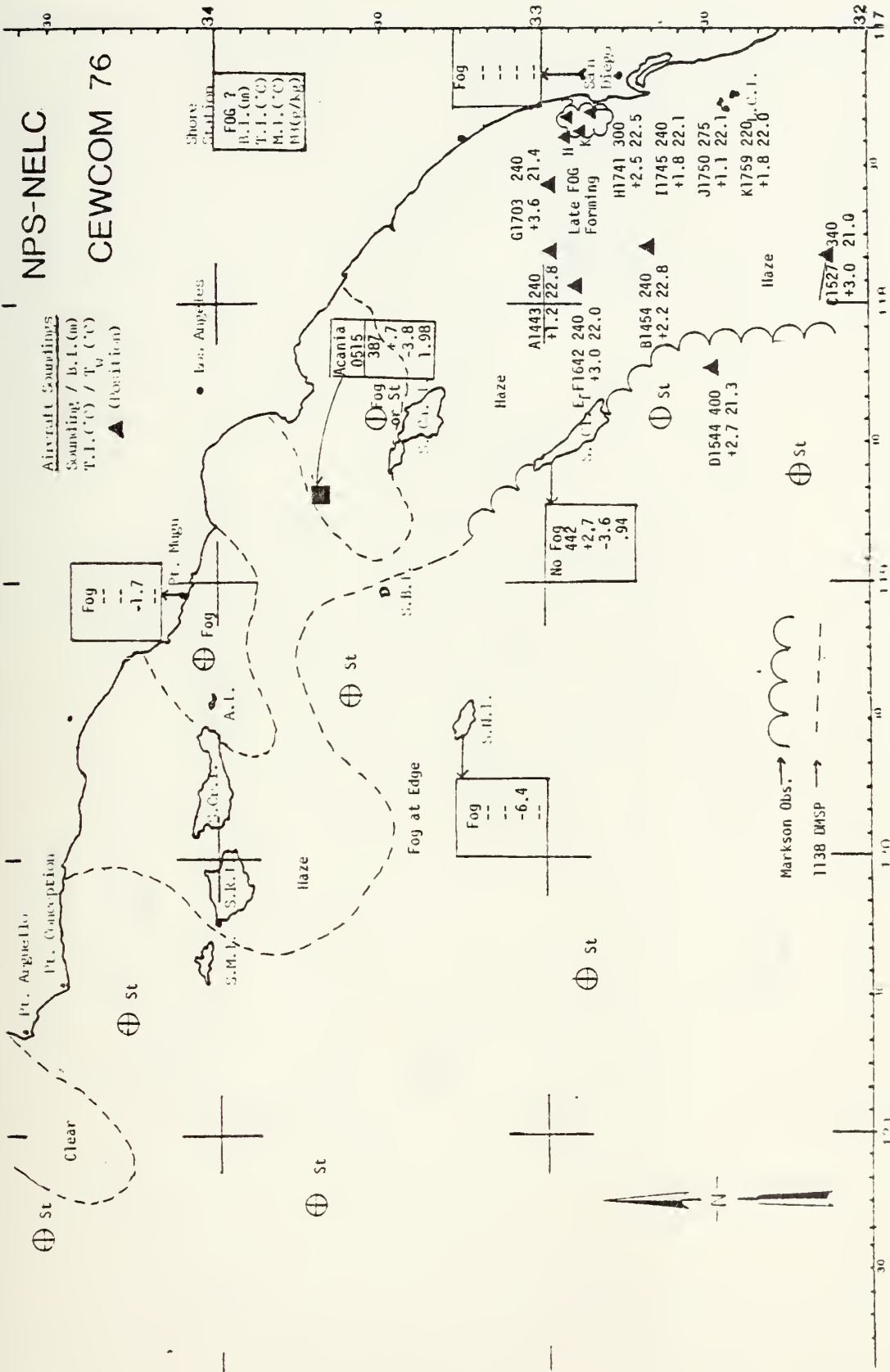Figure A-4-h   Indices and Weather Depiction

96

Figure A-4-i   Indices and Weather Depiction

Figure A-4-j   Indices and Weather Depiction

NPS-NELC

CEWCOM 76

Sensor – Barnes PRT-5
Platform – Aircraft
Altitude – 3 meters
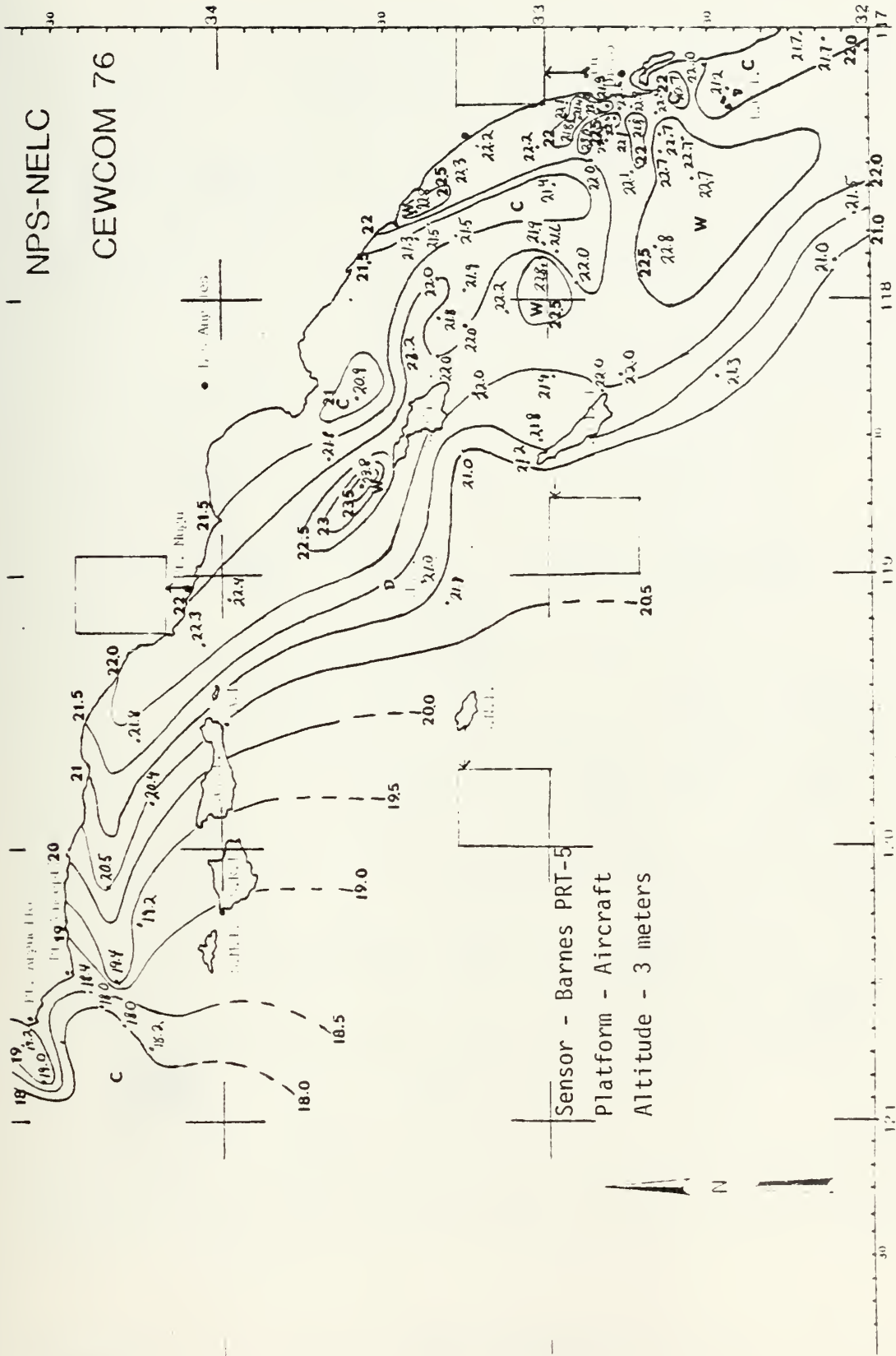
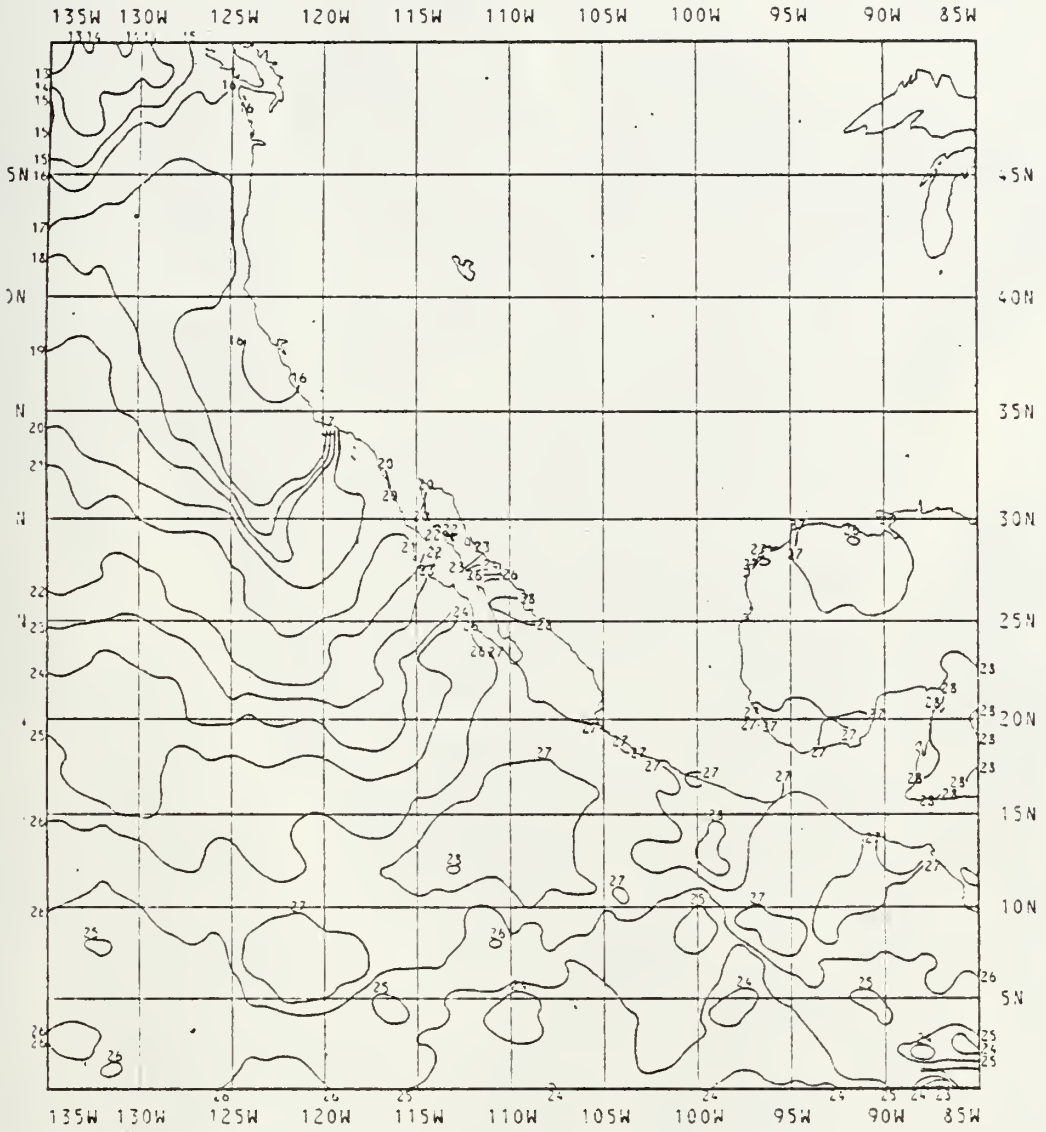Figure B-1   Aircraft Sea Surface Temperature Analysis

GOSSTCOMP SEA SURFACE TEMPERATURE

MN135W   10/12/76

Figure B-2   Weekly Satellite S.S.T.

Cloud

Figure B-3   The California Current
Satellite IR   11 Sept 74

Figure C-1   Fog downwind from Santa Catalina Island.
                  Top   1400 PDT, Bottom 1800 PDT (Photos
                  by R. Markson.)

Figure C-2   Catalina Island top half poking out
                    of haze layer.

Figure C-3   Common "Row Stratus" structure line up
                    parallel to the surface wind (Photos
                    by R. Markson.)

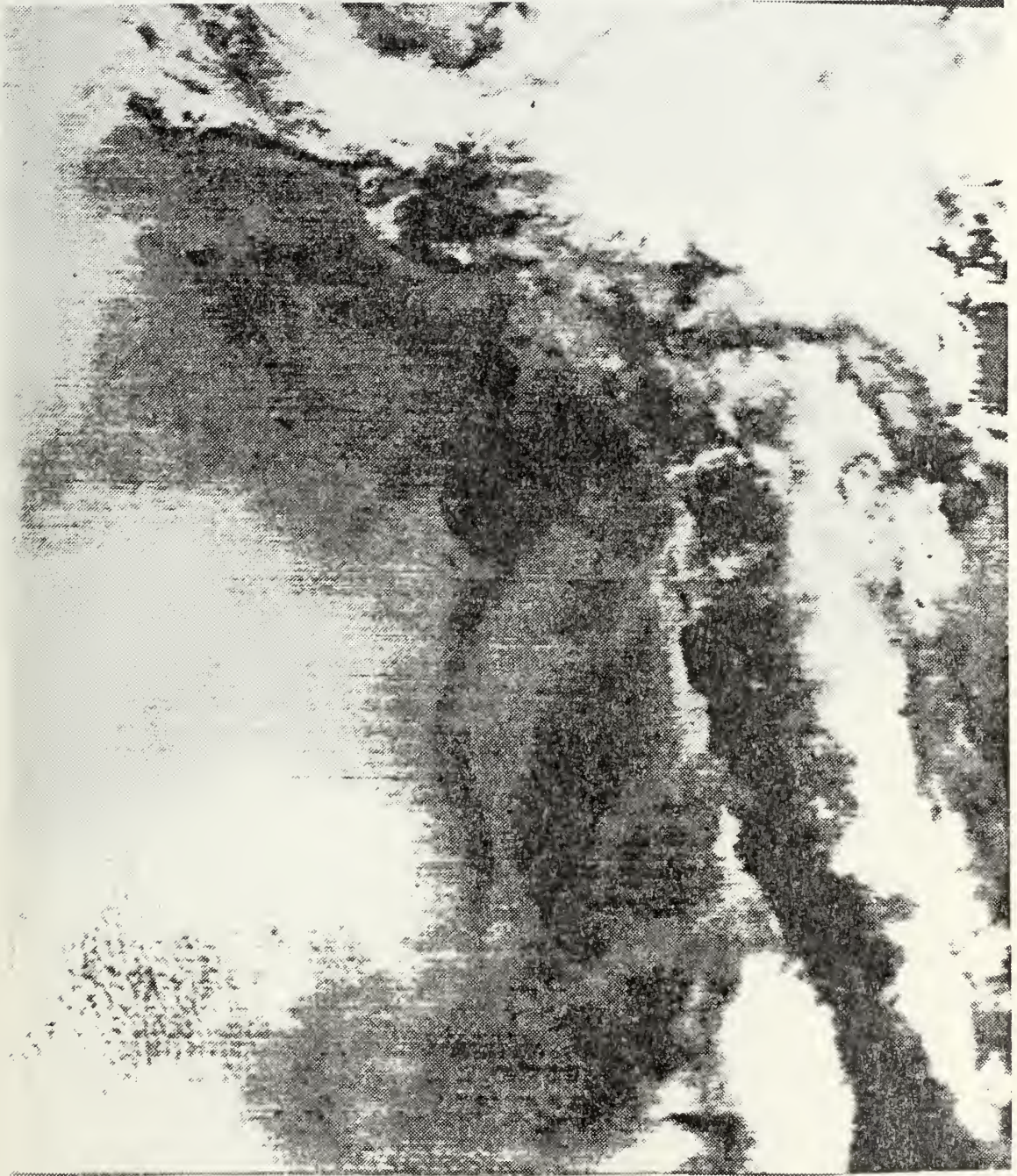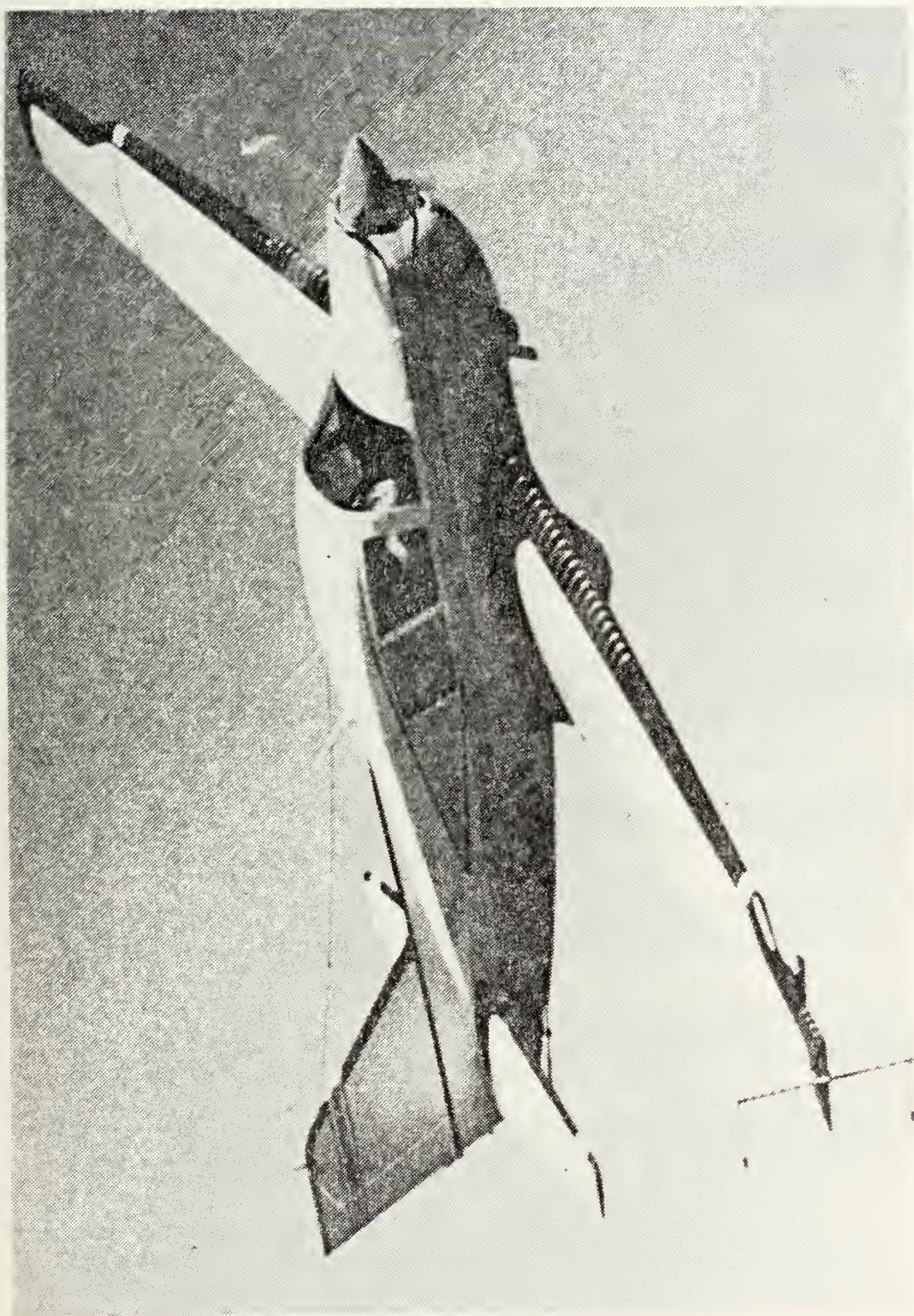Figure C-4   Satellite Visual Imagery on 8 October 1976
                    at 1552Z

Figure C-5   Satellite Infra-Red Imagery on 8 October
                    1976 at 1517Z

The Turbo-Bellanca Aircraft

Figure C-6

LIST OF REFERENCES

Blake, D., "Temperature Inversions at San Diego, as Deduced from Aerographical Observations by Airplane," _Monthly Weather Review_, v. 56, p. 221-224, June, 1928.

Beardsley, J.W., _Fog on the Central California Coast for 1973: Analysis of Trends_, M.S. Thesis, Naval Postgraduate School, Monterey, California, March, 1976.

Edinger, J.G., "Modification of the Marine Layer over Coastal Southern California," _Journal of Applied Meteorology_, v.2, p. 706-712, December, 1963.

Elliot, D.L. and O'Brien, J.J., "Observational Studies of the Marine Boundary Layer over an Upwelling Region," _Monthly Weather Review_, v. 105, p. 86-97, January, 1977.

Fleagle, R.G., Parrott, W.H. and Barad, M.L., "Theory and Effects of Vertical Temperature Distribution in Turbid Air," _Journal of Meteorology_, v.9, p. 53-60, February, 1952.

Fleagle, R.G., "A Theory of Fog Formation," _Journal of Marine Research_, v.7, n. 1, p. 43-49, 1953.

Fleet Weather Facility San Diego, California, _Climatological Study Southern California Operating Area_, prepared by Naval Weather Service Environmental Detachment, Asheville, North Carolina, March 1971.

Leipper, D.F., _Fog Forecasting on Coasts_, final report on the Fog Project, Office of Naval Research, Contract No. N6 oni-111, 31 August 1948.

Leipper, D.F., "Fog Development at San Diego, California," _Sears Foundation: Journal of Marine Research_, v.7, p. 337-346, 15 November 1948.

Leipper, D.F., "The Sharp Smog Bank and California Fog Development," _Bulletin of the American Meteorological Society_, v. 49, p. 354-358, April 1968.

Leipper, D.F., _The 1948 Coastal Fog Indices and CEWCOM 1976_, paper presented at Fifth Annual Marine Fog Investigation Program Review, Buffalo, New York, 5-6 April 1977.

Markson, Ralph, "Catalog of Temperature and Dew Point Soundings Obtained off Nova Scotia during Navy Fog Investigation, August 1975," prepared for _Office of Naval Research report on Marine Fog Cruise_, U.S.N.S. Hayes, 29 July - 28 August 1975.

Markson, Ralph, Report on Measurements during 1976 as part of the Marine Fog Investigation, presented at Fifth Annual Marine Fog Investigation Program Reivew, Buffalo, New York, 5-6 April 1977.

Naval Electronics Laboratory Center Technical Report 2000, Fog Related to Santa Ana Conditions in Southern California, by V.R. Noonkester and AGC L.E. Logue, p. 15-32, 5 November 1976.

Neiburger, M., Johnson, D.S. and Chein, C.W., "Studies of the Structure of the Atmosphere over the Eastern Pacific Ocean in Summer. I. The Inversion over the Eastern North Pacific Ocean," University of California Publications in Meteorology, v.1, p. 1-94, 1961.

NOAA (National Oceanic and Atmospheric Administration), Environmental Data Service, "daily weather maps," Weekly Series, 2-12 October 1976.

Oliver, D.A., Lewellen, W.S. and Williamson, C.G., "The Interaction Between Turbulent and Radiative Transport in the Development of Fog and Low-Level Stratus," prepared for Aeronautical Research Associates of Princeton, Inc., June, 1977.

Pacific Missile Range Report PMR-TP-71-2(U), Marine Layer over Sea Test Range, by J.G. Edinger and M.G. Wurtele, p. 1-78, 15 April 1971.

Renard, R.J., The Observation, Analysis, Forecasting and Climatology of Marine Fog, paper presented World Meteorological Organization Conference on the Applications of Marine Meteorology to the High Seas and Coastal Zone Development, Geneva, Switzerland, 22-26 November 1976.

Rosenthal, J., Point Mugu Forecaster's Handbook, Pacific Missile Range, Point Mugu, California, April 1972.

Schroeder, M.J. and others, "Marine Air Invasion of the Pacific Coast: A Problem Analysis," Bulletin American Meteorology Society, v. 48, p. 802-806, November 1967.

Taylor, G.I., The Formation of Fog and Mists, Quarterly Journal of the Royal Meteorological Society, v.43, July 1917.

White, L.J., "Sea Temperatures and Associated Data as Measured During CEWCOM," presented at a Thesis Seminar, Oceanography Department, at Naval Postgraduate School, Monterey, California, 18 March 1977.

INITIAL DISTRIBUTION LIST

No. Copies

1. Department of Oceanography, Code 68   10
   Naval Postgraduate School
   Monterey, CA 93940

2. Oceanographer of the Navy   1
   Hoffman Building No. 2
   200 Stovall Street
   Alexandria, VA 22332

3. Office of Naval Research   1
   Code 410
   NORDA
   NSTL, Station, MS 39529

4. Dr. Robert E. Stevenson   1
   Scientific Liaison Office, ONR
   Scripps Institution of Oceanography
   La Jolla, CA 92037

5. Library, Code 3330   1
   Naval Oceanographic Office
   Washington, D.C. 20373

6. SIO Library   1
   University of California, San Diego
   P. O. Box 2367
   La Jolla, CA 92037

7. Department of Oceanography Library   1
   University of Washington
   Seattle, WA 98105

8. Department of Oceanography Library   1
   Oregon State University
   Corvallis, OR 97331

9. Commanding Officer   1
   Fleet Numerical Weather Central
   Monterey, CA 93940

10. Commanding Officer   1
    Naval Environmental Prediction Research Facility
    Monterey, CA 93940

11. Department of the Navy   1
    Commander Oceanographic System Pacific
    Box 1390
    FPO San Francisco 96610

12. Defense Documentation Center   2
    Cameron Station
    Alexandria, VA 22314

13. Library (Code 0212)   2
    Naval Postgraduate School
    Monterey, CA 93940

14. Director   1
    Naval Oceanography and Meteorology
    National Space Technology Laboratories
    NSTL, Station, MS 39529

15. NORDA   1
    NSTL, Station, MS 39529

16. Mr. Roland Pilie   1
    Calspan Corporation
    Buffalo, New York 14221

17. Dr. Dee F. Taylor   1
    Naval Air Systems Command
    AIR-540
    Washington, D.C. 20360

18. Dr. James L. Kassner, Jr.   1
    Graduate Center for Cloud Physics Research
    University of Missouri
    Rolla, Missouri 65401

19. Dr. Dale F. Leipper, Code 68   1
    Department of Oceanography
    Naval Postgraduate School
    Monterey, CA 93940

20. LCDR J. W. Beardsley, USN   1
    72 Summit Drive
    Huntington, New York 11743

21. Mr. Gene Mack   1
    Calspan Corporation
    Buffalo, New York 14221

22. Mr. James Hughes   1
    Office of Naval Research
    Code 412
    Arlington, VA 22217

23. National Center for Atmospheric Research   1
    Library Acquisitions
    Boulder, Colorado 80301

24. Mr. Ray Noonkester   2
    Naval Ocean Systems Center
    San Diego, CA 92152

25. Mr. Ralph Markson   2
    Airborne Research Associates
    46 Kendal Common Road
    Weston, MA 02193

26. Dr. Ken Davidson, Code 63   1
    Department of Meteorology
    Naval Postgraduate School
    Monterey, CA 93940

27. LT Douglas Backes   3
    Route 1, P. O. Box 304
    Cold Spring, MN 56320

28. LT Frank McNab   1
    1275 Spruance Road
    Monterey, CA 93940

29. Mr. Jerry Norton, Code 68   1
    Department of Oceanography
    Naval Postgraduate School
    Monterey, CA 93940

30. Air Weather Service   1
    (AWVAS/TF)
    Scott AFB, Illinois 62225

31. Department of Meteorology, Code 63   1
    Naval Postgraduate School
    Monterey, CA 93940

32. Dr. Robert J. Renard, Code 63   1
    Department of Meteorology
    Naval Postgraduate School
    Monterey, CA 93940

33. Dr. Gordon E. Schacher, Code 61 Sq   1
    Department of Physics & Chemistry
    Naval Postgraduate School
    Monterey, CA 93940

34. Dr. Glenn H. Jung, Code 68   1
    Department of Oceanography
    Naval Postgraduate School
    Monterey, CA 93940

No. Copies

35. Dr. Alan Weinstein   1
    Stratiform Cloud Physics Fr.
    Meteorology Laboratory
    Department of the Air Force
    Air Force Cambridge Res. Lab.
    Laurence G. Hanscom Field
    Bedford, MA   01730

36. Dr. Pierre St. Amand   1
    Earth and Planetary Sci. Div.
    Code 602
    Department of the Navy
    Naval Weapons Center
    China Lake, CA   93555

37. Mr. Murray H. Schefer   1
    AIR-370C
    Naval Air Systems Command
    Washington, D.C. 20360

38. Dr. Lothar Ruhnke   1
    Naval Research Laboratory
    Code 8320
    Washington, D.C.   20390

39. Dr. Patrick Squires   1
    Desert Research Institute
    University of Nevada
    Reno, Nevada   89507

40. CDR Linda J. White   1
    Oceanographic Systems Pacific
    Box 1390
    FPO San Francisco, 96610